Biological Brain Age Prediction Using Machine Learning on Structural Neuroimaging Data: Multi-Cohort Validation Against Biomarkers of Alzheimer's Disease and Neurodegeneration stratified by sex

Irene Cumplido-Mayoral[1,2], Marina García-Prat[1], Grégory Operto[1,3,4], Carles Falcon[1,3,5], Mahnaz Shekari[1,2,3], Raffaele Cacciaglia[1,3,4], Marta Milà-Alomà[1,2,3,4], Luigi Lorenzini[6], Silvia Ingala[6], Alle Meije Wink[6], Henk JMM Mutsaerts[6], Carolina Minguillón[1,3,4], Karine Fauria[1,4], José Luis Molinuevo[1,*], Sven Haller[7], Gael Chetelat[8], Adam Waldman[9], Adam Schwarz[10], Frederik Barkhof[6,11,], Ivonne Suridjan[12], Gwendlyn Kollmorgen[13], Anna Bayfield[13], Henrik Zetterberg[14,15,16,17,18], Kaj Blennow[14,15], Marc Suárez-Calvet[1,3,4,19], Verónica Vilaplana[#20], Juan Domingo Gispert[#1,3,5]
ALFA study, EPAD study, ADNI study, OASIS study

1) Barcelonaβeta Brain Research Center (BBRC), Pasqual Maragall Foundation, Barcelona, Spain
2) Universitat Pompeu Fabra, Barcelona, Spain
3) IMIM (Hospital del Mar Medical Research Institute), Barcelona, Spain
4) CIBER Fragilidad y Envejecimiento Saludable (CIBERFES), Madrid, Spain
5) Centro de Investigación Biomédica en Red de Bioingeniería, Biomateriales y Nanomedicina (CIBER-BBN), Madrid, Spain
6) Department of Radiology and Nuclear Medicine, Amsterdam Neuroscience, Vrije Universiteit Amsterdam, Amsterdam UMC, Amsterdam, The Netherlands
7) CIRD Centre d'Imagerie Rive Droite, Geneva, Switzerland
8) Normandie Univ, UNICAEN, INSERM, U1237, PhIND "Physiopathology and Imaging of Neurological Disorders", Institut Blood and Brain @ Caen-Normandie, Cyceron, Caen, France
9) Centre for Dementia Prevention, Edinburgh Imaging, and UK Dementia Research Institute at The University of Edinburgh, Edinburgh, UK
10) Takeda Pharmaceutical Company Ltd, Cambridge, MA, USA
11) Institutes of Neurology and Healthcare Engineering, University College London, London, UK
12) Roche Diagnostics International Ltd, Rotkreuz, Switzerland
13) Roche Diagnostics GmbH, Penzberg, Germany
14) Institute of Neuroscience and Physiology, University of Gothenburg, Mölndal, Sweden
15) Clinical Neurochemistry Laboratory, Sahlgrenska University Hospital, Mölndal, Sweden
16) Department of Neurodegenerative Disease, UCL Queen Square Institute of Neurology, London, United Kingdom
17) UK Dementia Research Institute at UCL, London, United Kingdom
18) Hong Kong Center for Neurodegenerative Diseases, Hong Kong, China

19) Servei de Neurologia, Hospital del Mar, Barcelona, Spain
20) Department of Signal Theory and Communications, Universitat Politècnica de Catalunya, Barcelona, Spain
* Current affiliation: H.Lundbeck A/S, Copenhagen, Denmark

Corresponding authors

ABSTRACT (150 words)

Brain-age can be inferred from structural neuroimaging and compared to chronological age (brain-age delta) as a marker of biological brain aging. Accelerated aging has been found in neurodegenerative disorders like Alzheimer's disease (AD), but its validation against markers of neurodegeneration and AD is lacking. Here, imaging-derived measures from the UK Biobank dataset (N=22,661) were used to predict brain-age in 2,314 cognitively unimpaired (CU) individuals at higher risk of AD and mild cognitive impaired (MCI) patients from four independent cohorts with available biomarker data: ALFA+, ADNI, EPAD and OASIS. Brain-age delta was associated with abnormal amyloid-β, more advanced stages (AT) of AD pathology and *APOE*-ε4 status. Brain-age delta was positively associated with plasma neurofilament light, a marker of neurodegeneration, and sex differences in the brain effects of this marker were found. These results validate brain-age delta as a non-invasive marker of biological brain aging related to markers of AD and neurodegeneration.

INTRODUCTION

Age is the main risk factor for Alzheimer's Disease (AD) and most neurodegenerative diseases. However, the mechanisms underlying this association are still poorly understoodd (Fjell et al., 2014). Both normal aging and AD are associated with region-specific cerebral morphological changes characterized by the occurrence of atrophy (Bakkour et al., 2013; Fjell et al., 2014). Both aging and AD have differential and partially overlapping effects on specific regions of the cerebral cortex like, for instance, the dorsolateral prefrontal cortex (Bakkour et al., 2013; Fjell et al., 2014; Pichet Binette et al., 2020). Conversely, some regions are predominantly affected by age (e.g., calcarine cortex) and some others are predominantly affected by AD (e.g., medial temporal cortex) (Bakkour et al., 2013). A better understanding of the mechanistic links between the brain aging process and neurodegenerative diseases is an urgent priority to develop effective strategies to deal with their rising burden amid an ageing population (Franke & Gaser, 2019). Therefore, a growing amount of research is focusing on using neuroimaging techniques to develop a biomarker of biological brain aging. In this framework, the concept of brain-age has emerged as an appealing comprehensive marker that enables determining on an individual basis, the risk for age-associated brain diseases (James H. Cole et al., 2017; James H. Cole & Franke, 2017; Franke et al., 2010; Franke & Gaser, 2019). However, this is a challenging task because, even though the cerebral structural changes related to aging are well established, the older population is characterized by

substantial variation in neurobiological aging trajectories (J. H. Cole et al., 2018; Fjell et al., 2014).

Recently, machine learning techniques have gained popularity as brain-age prediction models (James H. Cole et al., 2017; Dafflon et al., 2020; de Lange et al., 2019; Franke & Gaser, 2019), due to their ability in identifying relevant data-driven patterns within complex data (Zhavoronkov et al., 2019). These models learn the association between chronological age and cerebral morphological features derived from structural magnetic resonance imaging (MRI) in healthy individuals, yielding a predicted brain-age for each individual. Individuals with a predicted brain-age higher than their chronological age may have an "older" brain than expected, whereas an individual with an estimated brain-age lower than their chronological age has a "younger" brain. Subtracting chronological age from estimated brain-age hence provides an estimate of accelerated brain aging, namely the brain-age delta. Recent literature has shown the adequacy of using a brain-age predicted measurement in the assessment of the clinical severity of AD, by finding higher brain-age deltas in AD and individuals with mild cognitive impairment (MCI) with respect to cognitively unimpaired (CU) individuals (Beheshti et al., 2018; Kaufmann et al., 2019). A higher brain-age delta has also been reported in other diseases, such as multiple sclerosis, epilepsy and psychiatric disorders, with respect to healthy controls (Beheshti et al., 2018; Kaufmann et al., 2019). In addition, brain-age delta has also been associated with other biological measures such as: lifestyle factors (James H. Cole, 2020), cognition (Beheshti et al., 2018; James H. Cole, 2020) hypertension (de Lange, et al., 2020) and prediction of mortality (J. H. Cole et al., 2018).

Even though these studies support the association of brain-age delta as a biomarker of biological aging with relevance to various brain diseases, there are no comprehensive studies validating this measurement in association with specific biological markers of AD pathology (*i.e.* Amyloid-β [Aβ] and tau pathology), neurodegeneration and cerebrovascular disease. This is a very relevant aspect since the recent AD research framework criteria defines AD as a biological construct, namely the presence of both abnormal Aβ (A+) and tau (T+) biomarkers, regardless of clinical manifestations(Jack et al., 2018). The term "Alzheimer's pathological change" is proposed whenever there is evidence of Aβ but not tau pathology (A+T-). The umbrella term "Alzheimer's *continuum*" includes both "Alzheimer's pathological change" (A+T-) and "Alzheimer's Disease" (A+T+). Under this definition, A-T+ individuals would not fall into the AD *continuum*. Then, under this framework, neurodegeneration biomarkers (N) and cognitive status (*i.e.* CU, MCI and dementia syndromes) are used to stage disease progression.

A recent study used brain-age measurements to identify amnestic MCI (aMCI), the typical clinical presentation of prodromal AD, from other individuals with MCI, by studying the association with AD risk factors such as apolipoprotein E (*APOE*) and Aβ(Huang et al., 2021). Another study focusing on the impact of training the brain-age prediction model in individuals with Aβ pathology (Aβ+) showed that CU Aβ+ individuals had a higher brain-age delta than CU Aβ- individuals (Ly et al., 2020). Nonetheless, there remains a need to study the associations between brain-age prediction and AD as well as neurodegeneration biomarkers in preclinical stages in different and independent cohorts and in a larger sample size. Moreover, given that female individuals have a higher AD prevalence compared to males (Nebel et al., 2018) and display different lifetime trajectories in the brain morphological features (Gennatas et al., 2017), it is of interest to determine the effect of sex on brain age delta and its interaction with AD

biomarkers. Literature describes sex differences in AD biomarkers, such as that females with abnormal Aβ who are *APOE*-ε4 carriers show greater subsequent increase in cerebrospinal fluid (CSF) tau than their male counterparts (Buckley et al., 2019), or that females with higher Aβ burden show higher entorhinal cortical tau than their male counterparts (Buckley et al., 2019). Conversely, levels of the neurodegeneration biomarker CSF neurofilament light (NfL) have been widely reported to be higher in males than in females (Mielke, 2020; Milà-Alomà et al., 2020). In line with this, AD risk factors are associated with greater brain aging in women than men (Subramaniapillai et al., 2021).

Therefore, in the present study, we aim to validate brain-age delta as a clinically relevant marker related to markers of AD and neurodegeneration. For this purpose, we determine the association between the predicted structural brain-age delta with biomarkers and risk factors for AD and neurodegeneration in non-demented individuals, as well as to study the effect of sex on these associations. We trained a model to predict the brain-age separately for females and males, using machine learning on imaging-derived measures of cortical thickness, cortical volume, and subcortical volume from the UK BioBank cohort (N=22,661). Using this model, we then estimated brain-age in four independent cohorts: ALFA+ (N=380), ADNI (N=719), EPAD (N=808) and OASIS (N=407). In each cohort, we studied the associations of brain-age delta with biomarkers of AD pathology (CSF Aβ and p-tau as continuous values, as well as categorized in AT stages), the *APOE*-ε4 genotype which is the main genetic risk factor for AD, neurodegeneration (CSF and plasma NfL), and small vessel disease (White Matter Hyperintensities [WMH]). Finally, we studied the sex differences in brain age prediction and the sex effects with these biomarkers on brain-age delta.

RESULTS

Participants' Characteristics

Table 1 summarizes the demographic characteristics of the cohorts included in the study. ADNI and EPAD cohorts included both CU and MCI individuals, while the UK BioBank, ALFA+ and OASIS cohorts only included CU individuals. Table 2 summarizes the variables used to study the associations with brain-age delta, which included biomarkers for AD (Aβ positron emission tomography [PET] and CSF Aβ and p-tau), neurodegeneration (CSF and plasma NfL), and cerebrovascular pathology (WMH on MRI), as well as the aging signature composite(Bakkour et al., 2013), both cross-sectional and longitudinally. The aging signature composite is a map of specific brain regions that undergo cortical thinning in normal aging, which has been used as a proxy measurement for brain aging. These validation variables were correlated with chronological age for all cohorts (see Supplementary Table 1). Some of the participants for ALFA+ (N=25), ADNI (N=116) and EPAD (N=71) fell into the A-T+ group, corresponding to non-AD pathologic change. Since our aim was to specifically validate the brain-age delta measurements in the AD *continuum*, we excluded these participants from subsequent analyses; and they are reported within Table 1 and Table 2 solely for descriptive purposes. In addition, the number of MCI individuals with available data of CSF NfL and of aging signature change was relatively low and, therefore, these variables were excluded from the analysis in MCI individuals.

Table 1. Sample demographics and characteristics separated by cohort and by diagnosis.

	CU					MCI	
Characteristics	**UK BioBank**	**ALFA+**	**ADNI**	**EPAD**	**OASIS**	**ADNI**	**EPAD**
	(n=22,661)	(n=380)	(n=284)	(n=653)	(n=407)	(n=435)	(n=155)
Age, years	64.54 (7.55)	60.61 (4.72)	71.42 (6.36)	64.96 (7.01)	69.07 (9.42)	71.09 (7.31)	69.08 (6.97)
Age range, years	[44, 81]	[48, 73]	[55, 89]	[50, 88]	[42, 89]	[55, 91]	[52, 88]
Female, n (%)	11,767 (51.92)	254 (60.76)	126 (50.00)	386 (59.11)	244 (59.95)	249 (50.00)	81 (47.74)
Education, years	17.75 (5.42)	13.43 (3.71)	16.54 (2.49)	14.83 (3.56)	15.93 (2.59)	16.23 (2.71)	14.17 (3.77)
***APOE*-ε4 carriers, n (%)**	6,334 (27.95)	221 (52.87)	72 (28.57)	217 (33.23)	118 (28.99)	218 (43.78)	60 (38.71)
MMSE	-	29.15 (0.95)	28.985 (1.24)	28.82 (1.40)	29.03 (1.31)	27.57 (2.19)	27.86 (1.97)

Notes: Data are expressed as mean (M) and standard deviation (SD) or percentage (%), as appropriate.
Abbreviations: *APOE*, apolipoprotein E; MMSE, Mini-Mental State Examination.

Table 2. Biomarkers separated by cohort and by diagnosis

	CU								MCI			
	ALFA+		ADNI		EPAD		OASIS		ADNI		EPAD	
BIOMARKERS	**N**	**Mean (SD)**	**N**	**Mean (SD)**	**N**	**Mean (SD)**	**N**	**Mean (SD)**	**N**	**Mean (SD)**	**N**	**Mean (SD)**
Centiloids	0	-	0	-	0	-	407	13.468 (28.138)	0	-	0	-
CSF Aβ42 (pg/mL) [a]	380	1318.059 (599.223)	284	1223.890 (556.648)	653	1403.617 (681.736)	0	-	435	986.248 (446.402)	155	1245.181 (741.756)
CSF p-tau (pg/mL)	380	16.289 (7.813)	283	22.234 (9.692)	627	18.326 (8.380)	0	-	434	26.490 (14.402)	151	24.715 (14.897)
CSF NfL (pg/mL) [b]	380	82.717 (29.124)	26	1052.444 (376.095)	0	-	0	-	48	1383.638 (918.231)	0	-
Plasma NfL (pg/mL)	368	10.519 (3.739)	184	35.843 (17.988)	0	-	0	-	404	38.157 (18.908)	0	-
WMH volume	360	0.045 (0.845)	240	-0.0085 (1.267)	456	0.038 (1.072)	0	-	458	-0.005 (1.229)	108	0.048 (1.076)
Aging signature [b]	360	2.387 (0.071)	240	2.284 (0.105)	456		0	-	458	2.251 (0.109)	0	-
Aging signature V2 [b]	187	2.376 (0.072)	45	2.299 (0.118)	0	-	0	-	46	2.257 (0.119)	0	-
Aging signature change $(V2 - V1/\Delta t)$ [b]	187	-0.003 (0.011)	45	-0.0007 (0.037)	0	-	0	-	46	-0.003 (0.050)	0	-

Notes: Data are expressed as mean (M) and standard deviation (SD) or percentage (%), as appropriate.
Amyloid-β status was defined by CSF (ALFA+, ADNI and EPAD) or amyloid PET (OASIS).
For ALFA+ and ADNI, we calculated the aging signature from MRI scans acquired 3 years later than the original MRI scan, called aging signature V2. Aging signature change was calculated as the difference in aging signature over these two MRI scans.

[a] Individuals that fell into the A-T+ group: 25 from ALFA+, 116 from ADNI and 71 from EPAD.
[b] As the number of MCI individuals with CSF NfL and aging signature change was relatively low, we excluded them from the following results.
Abbreviations: CSF, cerebrospinal fluid; NfL, neurofilament light; WMH, White Matter Hyperintensities.

Brain-Age Prediction and Chronological Age

We trained the prediction model using the UK BioBank cohort and tested the model using four independent cohorts (ALFA+, ADNI, EPAD and OASIS), as shown in Supplementary Fig. 1. Table 3 shows the prediction accuracy before and after age-bias correction for the combined female and male predictions. The average prediction accuracy of the model run on UK BioBank using ten-fold cross-validation as measured by the mean absolute error (MAE) and by Pearson's correlation were, originally, MAE=4.19 and R=0.71 and, after correction, MAE=2.95 and R=0.89 (Table 3 and Supplementary Fig. 2).

We then investigated the association of predicted brain-age with chronological age on each of the independent cohorts. All the cohorts showed a similar positive correlation and fitting performance metrics as measured by the mean absolute error (MAE), R and root mean squared error (RMSE) between chronological age and predicted brain-age. Correlation coefficients were not different between cohorts (P>0.05, for all comparisons, see Supplementary Table 2). As an example, after bias correction, the highest numerical difference was between ALFA+ and OASIS, with quite similar MAE=3.25 and R=0.729 and MAE=3.81 and R=0.910, respectively.

In order to study the effect of sex on brain age prediction, we also computed the performance metrics stratified by females and males (Supplementary Table 3 and 4). Correlations and fitting performance metrics were not significantly different between females and males (Pearson's r (William's test), P>0.05; RMSE (F-test) P>0.05), see Supplementary Table 5. Plots of the correlations between predicted brain-age and chronological age for females and males in each of the cohorts can be seen in the Supplementary Fig. 3.

Table 3. **Prediction metrics for all independent cohorts.**

Cohorts	Correlation with age		MAE (y)	R^2	RMSE
	R	P-value			
Before bias correction					
UK BioBank	0.712 (0.007)	**<0.001**	4.19 (0.07)	0.51 (0.03)	5.25 (0.08)
ALFA+	0.448	**<0.001**	4.31	0.20	4.18
ADNI	0.587	**<0.001**	7.21	0.34	5.47
EPAD	0.629	**<0.001**	4.63	0.40	5.62
OASIS	0.733	**<0.001**	6.99	0.54	6.42
After bias correction					
UK BioBank	0.898 (0.004)	**<0.001**	2.95 (0.10)	0.89 (0.01)	3.29 (0.10)
ALFA+	0.729	**<0.001**	3.25	0.53	3.99
ADNI	0.807	**<0.001**	4.47	0.65	5.47
EPAD	0.847	**<0.001**	3.29	0.72	4.07
OASIS	0.910	**<0.001**	3.81	0.82	4.83

The Pearson's correlation coefficient (R) between predicted brain-age and chronological age, R^2, root mean square error (RMSE), and mean absolute error (MAE) for UKBiobank and for each of the independent cohorts before and after bias correction. Age bias (Pearson's correlation between brain-age delta and chronological age) is also computed. For UKBiobank, the metrics, given as mean (standard deviation) are computed from 10-fold cross validation with 10 repetitions per fold.

Brain Regions Associated with Aging

We computed the SHapley Additive exPlanation (SHAP) values, which reflect the marginal contribution of each brain region to the brain-age prediction, using the UKBioBank dataset. SHAP values interpret the impact in the prediction of the values of volume or cortical thickness for a given brain region. In other words, they reflect the most important features that consistently influenced the prediction of brain-age and whether the decrease or increase of each region impacted into predicting a higher or lower brain-age. The SHAP values were computed separately for females and males. We compared the regions with higher SHAP values for females and males, and vice-versa, by averaging the SHAP values within each sex separately and then subtracting the mean SHAP of males to the mean SHAP of females.

There were regions whose SHAP values were high in both females and males, including the volumes of the amygdala, nucleus accumbens, cerebellar white matter, lateral ventricles and the insula, as well as the cortical thickness of the superior-temporal cortex. All the brain regions with consistent highest SHAP values for females and males are shown in Fig. 1a-b, as well as the effect of each region (larger or lower value) on predicting a higher brain-age. Conversely, the thickness of regions such as the transverse temporal cortex, the pars triangularis, the inferior parietal cortex and the left frontal pole thickness, as well as the volume of the left entorhinal cortex had higher SHAP values in females than in males, while the opposite occurred with the thickness of the left isthmus cingulate and the right cuneus and the cortical volume of the superior frontal and right rostral middle regions (Fig. 1c).

In Fig. 1d we can see the aging trajectories of three regions whose SHAP values were different for females and males. For example, the bi-lateral superior frontal volumes decreased more over the years within males than females. This result was seen as the interaction of sex with age ($P_{interatcion}<0.001$). We also found an interaction effect of sex and age for the isthmus cingulate thickness ($P_{\text{interatcion}}<0.001$), by which the thickness of males decreased more over the years than from the females. On the contrary, we also found regions, such as the middle temporal thickness, which followed the same trajectory over time for both sexes ($P_{\text{interaction}}=0.671$), but which was lower for females than for males ($P<0.001$).

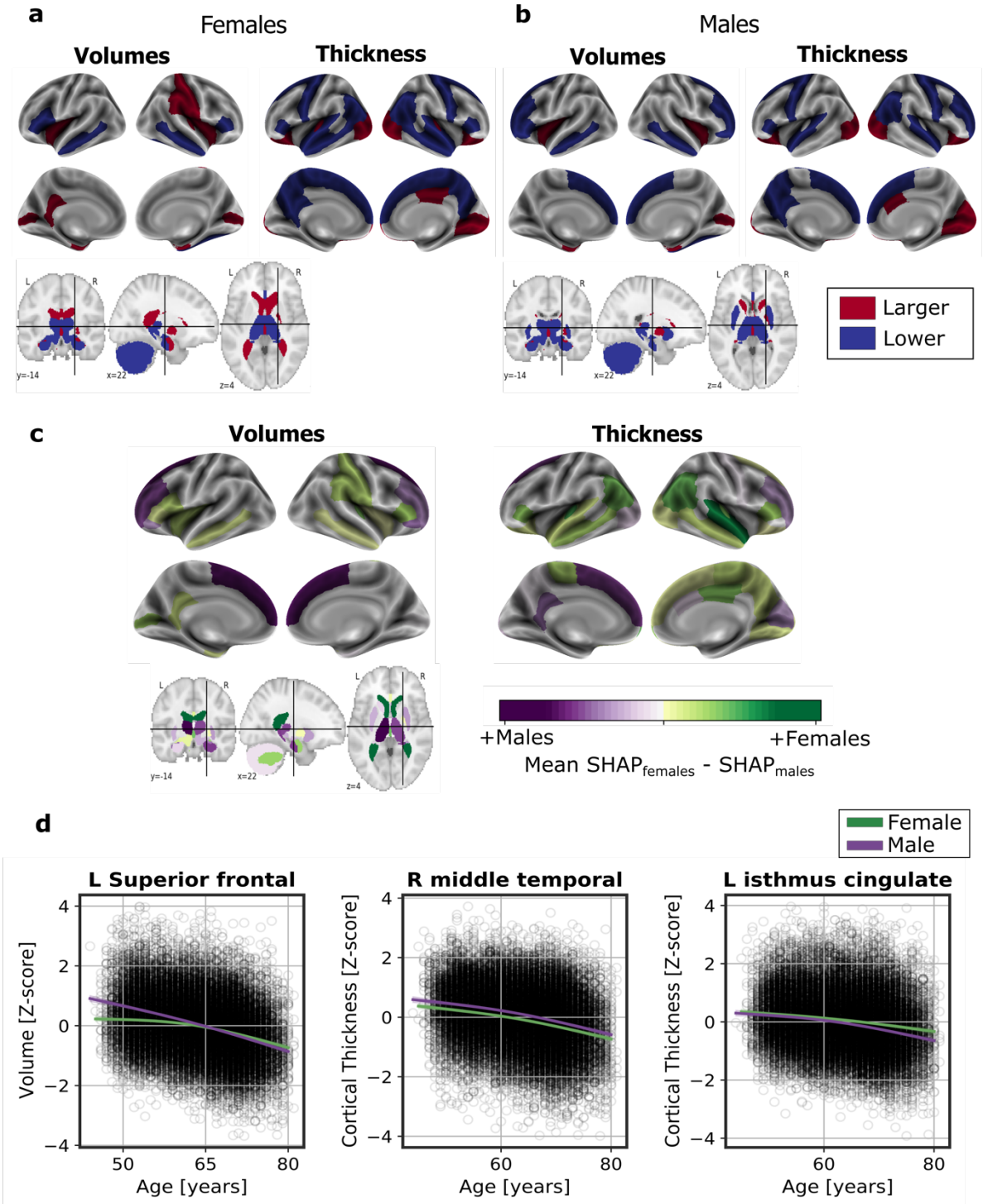

Figure 1. Significant SHAP-selected brain regions most important in prediction for **a** females and **b** males separately. Significance was studied by assessing the stability of the region's importance by performing subsampling of data over 1,000 permutations. Colored regions had a p-value<0.05 corrected for multiple comparisons using Bonferroni correction approach. Regions in red show larger volume or cortical thickness, while regions in blue show lower volume or cortical thickness. In **c**, the difference between the SHAP values of the significant SHAP-selected regions for females and males. In green, higher values for females and in red, higher for males. In **d**, examples of different aging trajectories for females and males of different significant SHAP-selected regions. For visualization purposes, nonparametric smoothing spline functions were used to fit the data.

Associations with AD biomarkers and risk factors

We studied the association between brain-age delta and AD biomarker classifications (Aβ status, AT stages) and *APOE*-ε4 status in all the independent cohorts pooled together, with a linear model adjusting for the effect of age and sex (Figure 2 and Table 4). Aβ status was defined by CSF (ALFA+, ADNI and EPAD) or amyloid PET (OASIS) using pre-established cut-off values (Hansson et al., 2018; Milà-Alomà et al., 2020; Salvadó et al., 2019; Schindler et al., 2018). Brain-age delta was higher in MCI with respect to CU individuals (P<0.001). In both CU and MCI, a higher brain-age delta was significantly associated with abnormal Aβ status (CU: P<0.001 and MCI: P<0.001) and with progressive AT stages (CU: P<0.001 and MCI: P<0.001) (see Table 4 and Supplementary Table 6 for more details). The mean brain-age delta values for the different Aβ status and AT stages can be found in Supplementary Table 7. The brain-age effect on AT stages was progressive, as that of the A+T- group was larger than that of A-T-, while the brain-age delta of A+T+ was larger than those of the other two previous stages (Table 4 and Fig 2a). Brain-age delta was also significantly associated with *APOE* status (CU: P<0.001 and MCI: P=0.029). In particular, *APOE*-ε4 carriers had larger brain-age deltas (i.e., older-appearing brains than expected for their chronological age) compared to *APOE*-ε33 individuals for both CU (β=0.105, P=0.032) and MCI (β=0.266, P=0.005) (see Table 4 and Figure 2). The mean brain-age delta values for the different *APOE* status can be found in Supplementary Table 7. These results were consistent with the results from the within-cohort analyses (see Supplementary Table 8).

We next studied the association between brain-age delta and AD biomarkers and risk factors stratified by sex (Table 5). In general, the same associations found with the whole sample was seen for females and males separately. However, although a higher brain-age delta was significantly associated with progressive AT stages both for females (CU: P<0.001 and MCI: P<0.001) and males (CU: P=0.009 and MCI: P<0.001), brain-age delta of A+T+ was significantly larger than those of the other two previous stages (A-T- and A+T-) in CU females (β=0.431, P=0.001) but not in CU males (β=0.139, P=0.364). We conducted regression analyses to test the interaction effect of sex and AT stages on CU brain-age delta. Although we found a trend by which the proportion of A+T+ with larger brain-age delta was larger in females than in males, the interaction effect was not significant ($P_{interaction}$=0.071).

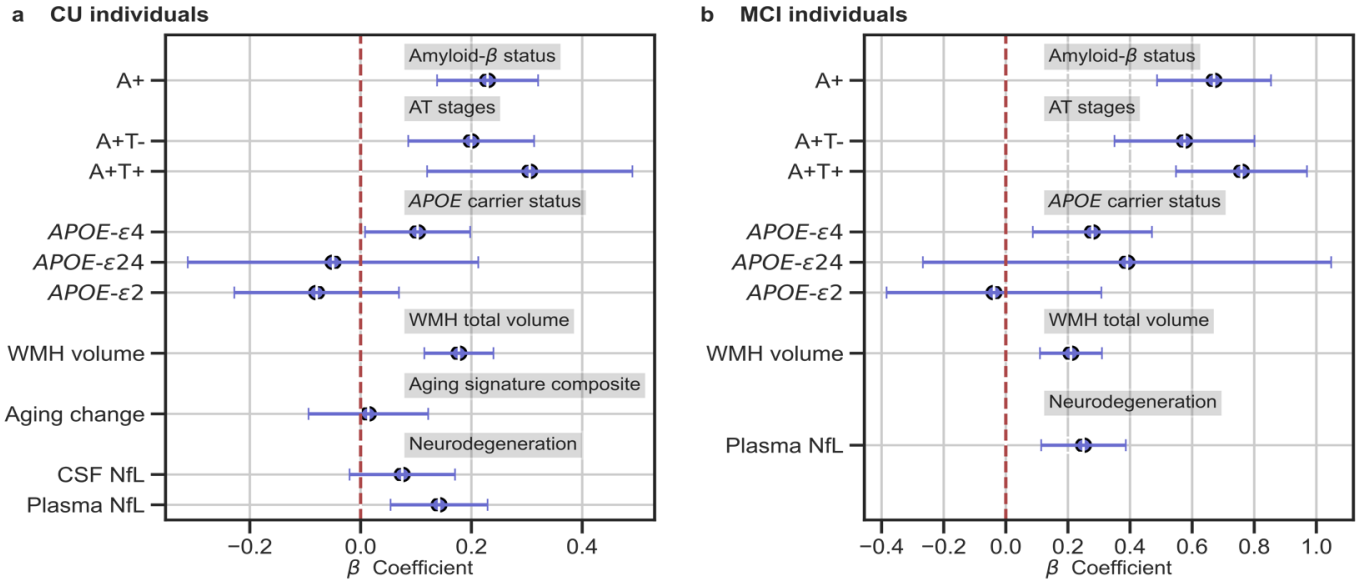

Figure 2. In **a** and **b**, the standardized associations ($\beta \pm$ 95% CI) between measures of brain-age delta validation variables for a) CU individuals and b) MCI individuals. Variables include AD biomarkers and risk factors: amyloid-**β** status, AT stages and APOE status; and neurodegeneration markers (available in ALFA+ and ADNI): CSF NfL, plasma NfL and aging signature change. The analyses included age and sex as covariates.

Table 4. Relationships between validation variables and brain-age delta for all CU and MCI individuals.

Model		*β*	SE	*P*-Value	[0.025	0.975]	N	Effect size
CU Individuals								
Amyloid-*β* pathology (ref: A-)		0.233	0.047	**<0.001**	0.140	0.325	1,634	0.222
Amyloid-*β* / Tau pathology (ref: A-T-)	**A+T-**	0.2023	0.059	**0.001**	0.087	0.318	1,162	0.205
	A+T+	0.310	0.096	**0.001**	0.122	0.498		0.311
***APOE* status (ref: *APOE*-ε33**	*APOE*-ε2	-0.081	0.077	0.295	-0.232	0.070	1,634	0.079
	APOE-ε4	0.105	0.049	**0.032**	0.008	0.201		0.100
	APOE-ε24	-0.051	0.136	0.795	-0.317	0.216		0.033
WMH volume †		0.171	0.030	**<0.001**	0.111	0.231	972	0.033
CSF NfL ‡		0.077	0.049	0.122	-0.021	0.173	378	0.006
Plasma NfL ‡		0.142	0.045	**0.002**	0.054	0.229	508	0.020
Brain Atrophy ‡		0.014	0.056	0.799	-0.096	0.124	152	0.000
Aging signature V1 ‡		-0.366	0.053	**<0.001**	-0.471	-0.261	152	0.175
Aging signature V2 ‡		-0.302	0.053	**<0.001**	-0.407	-0.198	152	0.120
MCI Individuals								
Amyloid-*β* pathology		0.640	0.089	**<0.001**	0.465	0.816	218	0.665
Amyloid-*β* / Tau pathology (ref: A-T-)	**A+T-**	0.550	0.109	**<0.001**	0.334	0.765	218	0.581
	A+T+	0.7245	0.107	**<0.001**	0.523	0.926		0.722
***APOE* status (ref: *APOE*-ε33**	*APOE*-ε2	-0.036	0.168	0.829	-0.367	0.294	218	0.036
	APOE-ε4	0.266	0.093	**0.005**	0.083	0.450		0.272
	APOE-ε24	0.372	0.319	0.244	-0.255	1.000		0.349
WMH volume		0.222	0.054	**<0.001**	0.117	0.327	191	0.040
Plasma NfL ¦		0.242	0.067	**<0.001**	0.110	0.374	134	0.043

Notes: Relationships between validation variables and Brain-Age delta from all CU pooled subjects (including ALFA+, ADNI, EPAD and OASIS) and all MCI pooled subjects (including ADNI and EPAD). Results given by the linear model: brain-age delta ~ each variable + chronological age + sex. The regression coefficients (β), standard errors (SE), P-value, 95% Confidence Interval, number of individuals (N) and effect size are depicted for each variable.
Significant values (P<0.05) are marked in bold.
Effect size in categorical variables was calculated as Cohen's D, while Cohens f^2 was calculated for continuous measurements. Amyloid-β status was defined by CSF (ALFA+, ADNI and EPAD) or amyloid PET (OASIS). MCI individuals only contained individuals from ADNI and EPAD.
† Contains data from ALFA+, ADNI and EPAD.
‡ Contains data from ALFA+ and ADNI.
¦ Contains data from ADNI.
Abbreviations: APOE, apolipoprotein E; WMH, White Matter Hyperintensities; CSF, cerebrospinal fluid; NfL, neurofilament light; ref, reference.

Associations with neurodegeneration biomarkers

We next tested the associations between brain-age delta and neurodegeneration biomarkers (Fig. 2 and Table 4). CSF NfL, plasma NfL and longitudinal change of the aging signature were available in ALFA+ and ADNI. The positive associations between brain-age deltas and plasma NfL were significant within the CU (β=0.142, *P*=0.002) and MCI individuals (β=242, *P*<0.001). CSF NfL was not significantly associated with brain-age delta (β=0.077, *P*=0.122). The aging signature composite at both visits was negatively associated with brain-age delta (Visit 1: β=-0.366, *P*<0.001 and Visit 2: β=-0.302, *P*<0.001). That is, larger brain-age delta was associated with reduced cortical thickness in aging-vulnerable regions. However, the association between the longitudinal change in the aging signature and brain-age delta was not statistically significant (β=0.014, *P*=0.799).

We next studied the association between brain-age delta and neurodegeneration biomarkers stratified by sex (Table 5). The associations between brain-age delta and CSF NfL were significant within the CU females (β=0.131, *P*=0.042), but not within the CU males (β=-0.004, *P*=0.959). However, the interaction effect of sex and CSF NfL on CU brain-age delta (Fig. 3a) did not reach significance ($P_{interaction}$=0.170). In the same line, the associations between brain-age delta and plasma NfL were significant within the CU and MCI females (CU: β=0.193, *P*=0.001 and MCI: β=0.342, *P*=0.001), but not within the males (CU: β=0.079, *P*=0.254 and MCI: β=0.157, *P*=0.086). The interaction effect of sex and plasma NfL on brain-age delta (Fig. 3a) revealed a trend within CU individuals, by which, although not significant, plasma NfL was larger on females when the brain-age delta showed larger values (older-appearing brain) than in males (CU: $P_{interaction}$=0.092 and MCI: $P_{interaction}$=0.194).

In addition, we tested for the interaction effect of age and these biomarkers on brain-age delta. We found a significant interaction effect of age and CSF NfL on CU brain-age delta ($P_{interaction}$< 0.001) within the CU individuals (Fig 4a), by which the measures of CSF NfL were higher with age and with larger brain-age deltas (older-appearing brain). When stratifying by sex, this interaction effect of age was seen in females ($P_{interaction}$< 0.001), but not in males ($P_{interaction}$=0.241). Regarding plasma NfL (Fig. 4b), although we found a similar trend by which the measures of plasma NfL were higher with age and with larger brain-age deltas for CU and MCI individuals, the interaction effects were not significant (CU: $P_{interaction}$=0.136 and MCI: $P_{interaction}$=0.145). When stratifying by sex, this interaction effect of age was seen in CU females ($P_{interaction}$<0.016) and not in CU males ($P_{interaction}$=0.656). On the contrary, this interaction effect of age and plasma NfL on brain-age delta was seen in MCI males ($P_{interaction}$<0.017) and not in MCI females ($P_{interaction}$=0.621).

Associations with markers of cerebrovascular disease

We lastly tested the associations between brain-age delta and markers of cerebrovascular disease WMH; WMH data were available in ALFA+, ADNI and EPAD. In both CU and MCI, brain-age delta was significantly associated with WMH (CU: β=0.171, *P*<0.001 and MCI: β=0.222, *P*<0.001) (see Table 4). These results were consistent with the results from the within-cohort analyses (see Supplementary Table 7).

When studying the association between brain-age delta and WMH stratified by sex (Table 5) we found that the brain-age delta was positively associated with WMH both in CU females (β=0.202, P<0.001) and CU males (β=0.132, P=0.007). The interaction effect of sex and WMH on CU brain-age delta (Fig. 3a) was not significant ($P_{interaction}$=0.182). Conversely, we found that the brain-age delta was positively associated with WMH MCI males (β=0.154, P<0.001), but not in females (β=0.140, P=0.100). The interaction effect of sex and WMH on MCI brain-age delta (Fig. 3b) was also not significant ($P_{interaction}$=0.112).

Table 5. Relationships between validation variables and brain-age delta st ratified by sex for all CU and MCI individuals.

Model		Females					Males				
		β	**SE**	***P*-Value**	**N**	**Effect size**	***β***	**SE**	***P*-Value**	**N**	**Effect size**
CU Individuals											
Amyloid-*β* pathology (ref: A-)		0.224	0.063	**<0.001**	966	0.226	0.2434	0.072	**0.001**	668	0.246
Amyloid-*β* / Tau pathology (ref: A-T-)	**A+T-**	0.197	0.078	**0.012**	688	0.191	0.206	0.091	**0.024**	474	0.208
	A+T+	0.431	0.123	**0.001**		0.425	0.139	0.154	0.367		0.142
***APOE* status (ref: *APOE*-ε33**	*APOE*-ε2	-0.1301	0.104	0.211	966	0.128	-0.019	0.115	0.869	668	0.018
	APOE-ε4	0.081	0.064	0.203		0.080	0.130	0.079	0.098		0.122
	APOE-ε24	-0.001	0.187	0.998		0.001	-0.126	0.200	0.532		0.117
WMH volume †		0.202	0.039	**<0.001**	580	0.046	0.132	0.049	**0.007**	392	0.019
CSF NfL ¥		0.131	0.064	0.042	228	0.019	-0.004	0.078	0.959	150	0.000
Plasma NfL ‡		0.1923	0.059	**0.001**	298	0.037	0.079	0.069	0.254	210	0.006
Brain Atrophy ‡		0.073	0.074	0.328	171	0.005	-0.074	0.087	0.400	102	0.007
Aging signature V1 ‡		-0.410	0.067	**<0.001**	171	0.223	-0.301	0.092	**0.001**	102	0.109
Aging signature V2 ‡		-0.356	0.069	**<0.001**	171	0.159	-0.229	0.085	0.009	102	0.072
MCI Individuals											
Amyloid-*β* pathology		0.714	0.130	**<0.001**	217	0.752	0.5612	0.124	**<0.001**	286	0.578
Amyloid-*β* / Tau pathology (ref: A-T-)	**A+T-**	0.558	0.175	**0.002**	214	0.576	0.509	0.175	**<0.001**	284	0.529
	A+T+	0.8156	0.146	**<0.001**		0.818	0.626	0.145	**<0.001**		0.626
***APOE* status (ref: *APOE*-ε33**	*APOE*-ε2	0.006	0.295	0.984	217	0.006	-0.044	0.209	0.834	286	0.041
	APOE-ε4	0.270	0.142	0.06		0.283	0.259	0.126	**0.041**		0.259
	APOE-ε24	0.3278	0.418	0.435		0.348	0.415	0.812	0.417		0.406
WMH volume		0.140	0.085	0.100	181	0.154	0.291	0.070	**<0.001**	252	0.069
Plasma NfL¦		0.342	0.098	**0.001**	128	0.097	0.157	0.091	0.086	173	0.017

Notes: Relationships between validation variables and Brain-Age delta from all CU pooled subjects (including ALFA+, ADNI, EPAD and OASIS) and all MCI pooled subjects (including ADNI and EPAD). Results given by the linear model: brain-age delta ~ each variable + chronological age + sex. The standardized regression coefficients (β), standard errors (SE), P-value, 95% Confidence Interval, number of individuals (N) and effect size are depicted for each variable. Significant values (P<0.05) are marked in bold. Effect size in categorical variables was calculated as Cohen's D, while Cohens f^2 was calculated for continuous measurements. Amyloid-β status was defined by CSF (ALFA+, ADNI and EPAD) or amyloid PET (OASIS).

† Contains data from ALFA+, ADNI and EPAD.

‡ Contains data from ALFA+ and ADNI.

¦ Contains data from ADNI.

Abbreviations: APOE, apolipoprotein E; WMH, White Matter Hyperintensities; CSF, cerebrospinal fluid; NfL, neurofilament light; ref, reference.

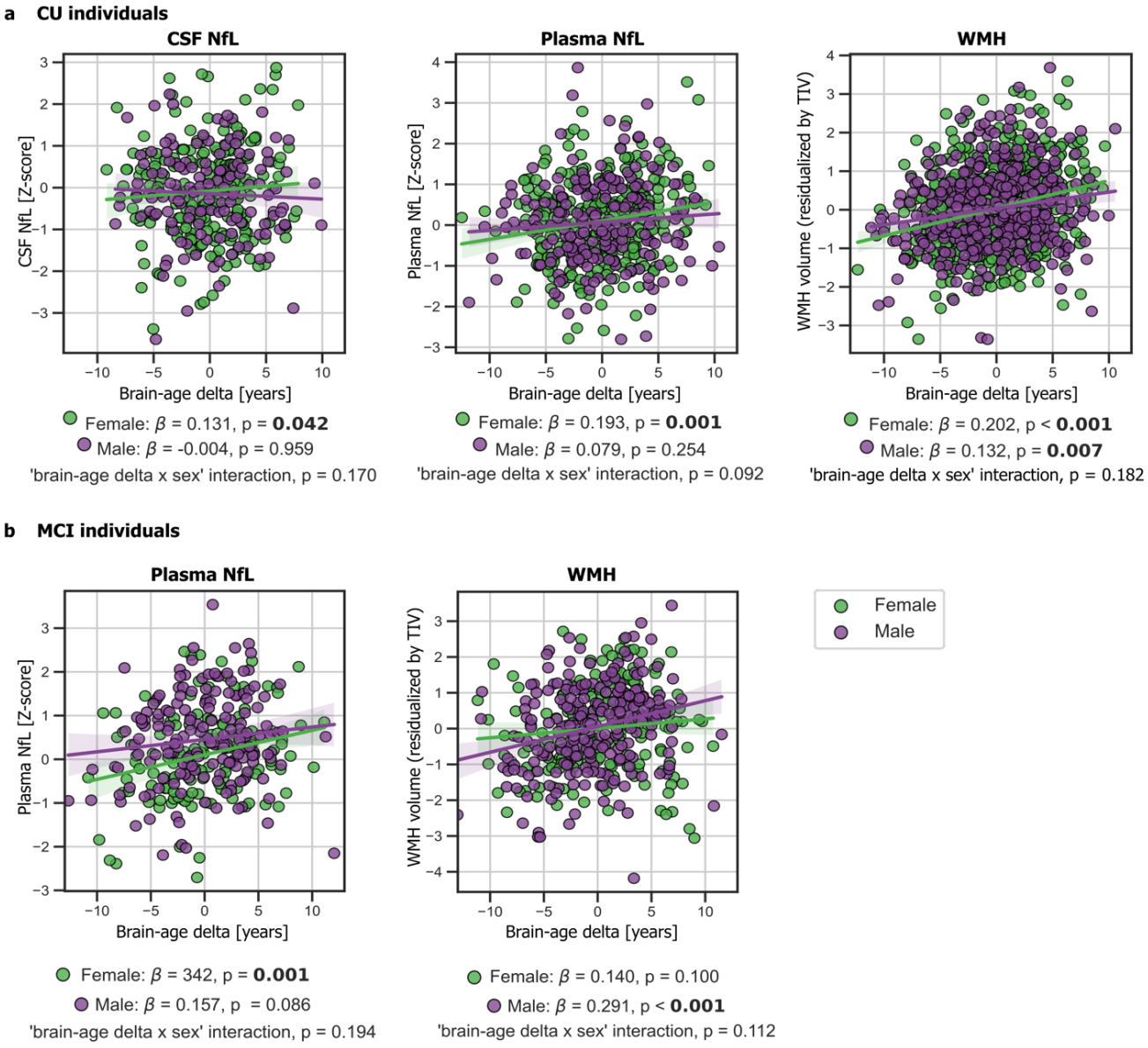

Figure 3. In **a** and **b**, the associations of brain-age delta and validation variables stratified by sex for a) CU individuals and b) MCI individuals. Scatter plots representing the associations of CSF NfL, plasma NfL and WMH with brain-age delta in females (green) and males (red). Each point depicts the value of the validation bioamarkers of an individual and the solid lines indicate the regression line for each of the groups. The standardized regression coefficients (β) and the P-values are shown and were computed using a linear model adjusting for age and sex. Additionally, we also computed the "brain-age delta x sex" interaction term.

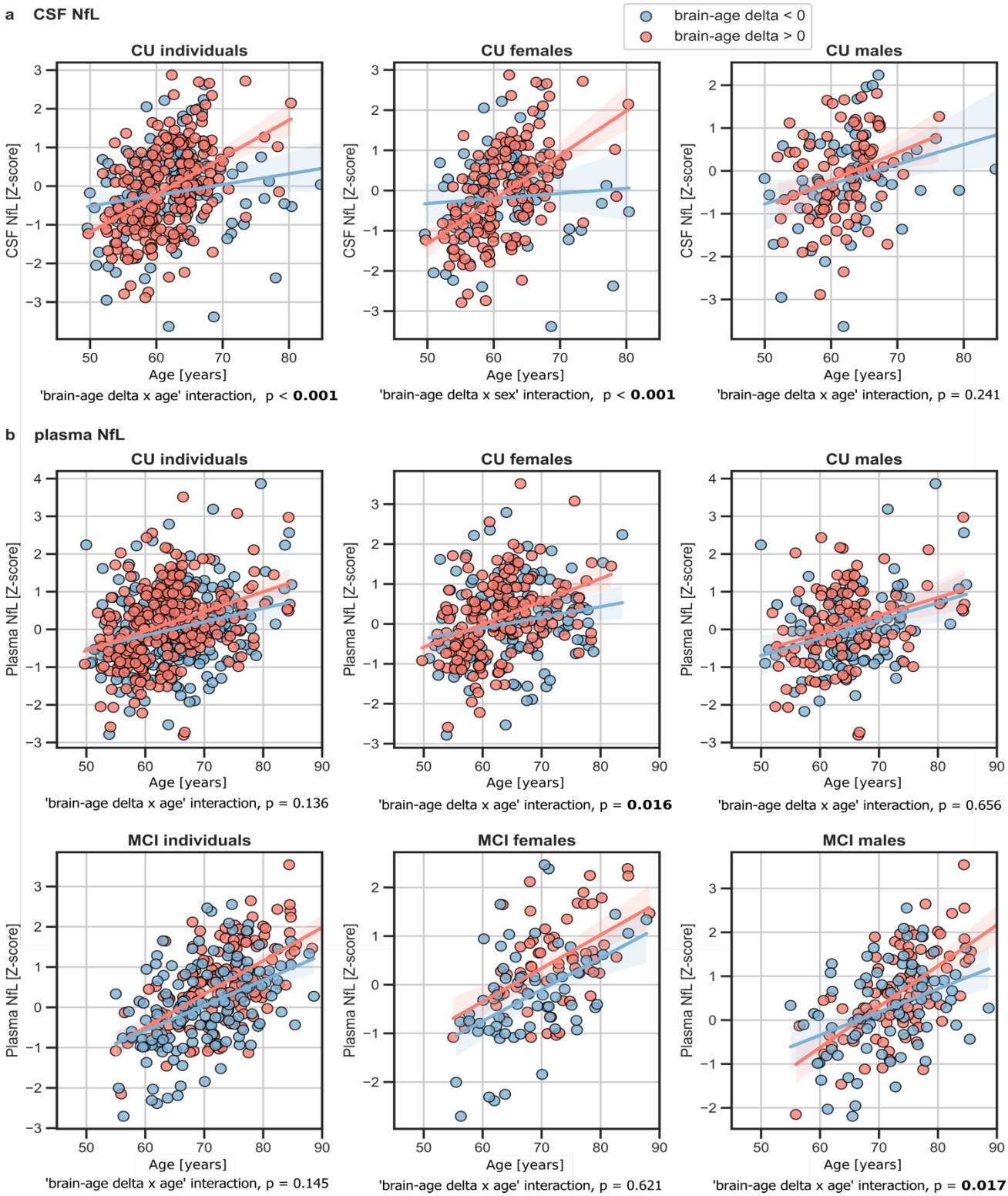

Figure 4. The associations of brain-age delta and **a** CSF NfL and **b** plasma NfL for all CU and, when available, MCI individuals. Scatter plots representing the associations of CSF NfL, plasma NfL and WMH with age in accelerated brain aging (purple) and decelerated brain aging (green). Each point depicts the value of the validation bioamarkers of an individual and the solid lines indicate the regression line for each of the groups. The regression coefficients (β) and the P-values are shown and were computed using a linear model adjusting for age and sex. Additionally, we also computed the "brain-age delta x sex" interaction term.

DISCUSSION

In this study, we show that, in non-demented individuals, the predicted brain-age delta is associated with specific AD biomarkers (amyloid-β PET, CSF Aβ42 and CSF pTau) and risk factors (*APOE* genotype), as well as with unspecific neurodegeneration biomarkers (plasma NfL), and markers of cerebrovascular disease (WMH volume). Our results also indicate that there are sex differences in the development of brain aging trajectories. Taken together, our findings validate the use of machine learning predicted brain-age deltas as biomarkers of brain aging and AD pathology.

We have studied, to our knowledge for the first time, the associations between brain-age delta and different biomarkers of AD pathology and neurodegeneration in CU individuals. We are aware of the complexity of disentangling the effects of aging and pathology in brain aging. In this work, we do not aim to disentangle to what extent the brain structural differences are caused by AD pathology (as measured by the biomarkers that we study) or aging. Here, we show that an unspecific estimation of biological brain aging, agnostic of the underlying mechanisms is associated with the specific biological process of AD.

Regarding the associations with AD biomarkers and risk factors, regression analyses revealed significant positive associations of brain-age delta with increased Aβ pathology and with AT stages for CU and MCI individuals. We also found significant associations with *APOE* status in the CU and MCI individuals, in which larger brain-age deltas were associated with the presence of *APOE*-ε4 allele. This result is in line with previous literature that has shown that *APOE*-ε4 carriership may accelerate AD-related brain atrophy (Evans et al., 2014; Filippini et al., 2011), as accelerated brain aging has also been found in MCI and AD patients (Beheshti et al., 2018; Kaufmann et al., 2019). The association of brain-age delta with *APOE*-ε4 was also previously studied, for which significant associations were found in MCI individuals (J. H. Cole et al., 2018; Löwe et al., 2016). Taken together, our results advocate for an effect of *APOE*-ε4 in physiological brain aging, albeit of a lesser magnitude than when AD pathology is present. These results with AD biomarkers and risk factors were highly reproducible in within-cohort analyses.

With the aim of studying the associations between brain-age delta and neurodegeneration, we computed the associations with NfL, a marker of neuro-axonal damage (Khalil et al., 2018) which can be measured both in CSF and in plasma, and with longitudinal changes in the aging signature composite as marker of age-related brain atrophy. The particular use of NfL in this context is supported by its correlation with age throughout the lifespan, as well as its strong association with all-cause mortality in the elderly (Kaeser et al., 2021). We found significant positive associations between brain-age delta and plasma NfL both in CU and MCI individuals, but we did not find significant associations between CSF NfL and CU brain-age delta. Even though we found NfL to be positively associated with chronological age in CU individuals, in line with previous studies (Beheshti et al., 2018; Kaufmann et al., 2019; Khalil et al., 2020; Milà-Alomà et al., 2020), the expected annual change of NfL in CU individuals whose mean age range was 65 years old is around 3.5% (Khalil et al., 2020). Therefore, we expected to find weak associations with brain-age delta. Still, we found a significant interaction effect of age and CSF NfL on CU brain-age delta, for which the individuals with larger brain-age delta had increased CSF NfL over the years, whereas the decelerated ones remained more stable. This trend was also seen in plasma NfL for CU and MCI individuals, although the interaction did not reach

significance. Taken together, a strong association between brain-age delta and plasma NfL was observed across all individuals whereas the association on CU brain-age delta and CSF NfL was milder and could only be detected as an interaction with age. Overall, these mild associations between brain-age delta and NfL suggest that the morphological effects of aging in the brain are not fully driven by neurodegeneration. In this regard, it is worth noting that cortical thinning with age has also been linked to loss of volume of the neuropil and other non-neuronal processes which are not necessarily implicated in neurodegeneration (Vidal-Pineiro et al., 2020).

We also studied the associations between brain-age delta and cerebrovascular disease. Regression analyses revealed significant associations of brain-age delta with increased WMH for both CU and MCI individuals. These results were expected, as the increase in WMH with age has been previously studied (Maniega et al., 2015) and it has been shown that individuals with high WMH burden display spatial patterns of atrophy that partially overlap with those of brain aging (Brugulat-Serrat, Salvadó, et al., 2020; Habes et al., 2016). In addition, WMH have been linked to cognitive dysfunction and dementia (Brugulat-Serrat, Salvadó, et al., 2020; Brugulat-Serrat, Salvadó, et al., 2020; Maniega et al., 2015) and a potential pathway has been proposed, in which small vessel cerebrovascular disease affects cognition by promoting neurodegenerative changes (Rizvi et al., 2018). In summary, our results support an effect of cerebrovascular disease in physiological brain aging.

Brain structure aging-associated changes have been widely studied (Bakkour et al., 2013; Fjell et al., 2014). In our study, the brain regions that had highest impact on the machine learning prediction were similar to regions previously mentioned in literature (Arenaza-Urquijo et al., 2019; Bakkour et al., 2013). We found an overlap between some of our selected regions and regions included in the aging signature for both females and males, such as the precentral sulcus, insula, superior frontal and rostral middle frontal regions. In addition, the effect of sex on age-related changes in brain structure has also been studied in the recent years, with some studies reporting age–sex interactions in volumes of certain brain structures (Coffey et al., 1998; DeCarli et al., 2005), and others not finding such interactions (Greenberg et al., 2008). In our study, we found that, even though most of the regions with highest impact were the same for males and females, there were some regions that were sex specific. In particular, we found reduction in the superior-frontal, isthmus-cingulate and pars orbitalis regions within males and regions such as inferior-parietal, pars triangularis and paracentral within females. Most of these sex-specific regions were in concordance with previous studies (Armstrong et al., 2019; Podgórski et al., 2021)**.** The mechanisms underlying these sex-specific brain aging differences are not well-known. Sexual hormones such as estrogen, progesterone and androgen could play a role in brain atrophy (Armstrong et al., 2019); in the WHIMS-MRI study (Resnick et al., 2009), women under menopausal hormone therapy were associated with greater brain atrophy. Others, however, have proposed that estrogen and progesterone may play a protective effect in women (Armstrong et al., 2019; Green & Simpkins, 2000). Other possible biological mechanisms influencing these results could be developmental (Baron-Cohen et al., 2005) or the influence of a greater presence of adverse lifestyle-related factors in men (DeCarli et al., 2005).

In line with the effect of sex on age-related changes in brain structure, we studied the effect of sex on the associations between brain-age delta and the above-mentioned variables. Regarding the AD biomarkers and risk factors, we found that the association

between brain-age delta and a larger proportion of A+T+ was only seen in females for the CU individuals, but the interaction effect of sex and AT stages on brain-age delta was not significant. Regarding the neurodegeneration variables, we found a mild positive association between brain-age delta and CSF NfL in CU females, as well as a stronger positive association between brain-age delta and plasma NfL in CU and in MCI females. These associations were not seen in their male counterparts. However, the interaction effect of sex and CSF and plasma NfL on CU and MCI brain-age delta was not significant. In addition, we found a significant interaction effect of age and CSF and plasma NfL on brain-age delta, for which the CU females with larger brain-age delta had increased CSF and plasma NfL over the years, whereas the decelerated ones remained more stable. On the contrary, we found an effect of age interaction with plasma NfL on brain-age delta in MCI males, but not in MCI females. These results were expected, as females have higher chances of developing neurodegeneration and have showed to undergo faster cognitive decline than males (Ferretti et al., 2018). Although the role of sex hormones still needs to be clarified, it has been suggested that the menopausal drop of estrogen increases vulnerability to neurological events (Green & Simpkins, 2000; Maioli et al., 2021). On the contrary, results suggest that morphological effects of aging in the CU males' brain are not fully driven by neurodegeneration, although these effects might increase with older age in MCI males. Lastly, regarding the cerebrovascular disease biomarkers, we found a positive association between brain-age delta and WMH for both CU females and males, while no interaction effect of sex was found. Conversely, in MCI individuals, we only found positive associations between brain-age delta and WMH on males, but no interaction effect of sex was found in MCI individuals. Overall, we found sex differences in the associations between brain-age delta and markers of neurodegeneration and cerebrovascular disease. NfL was only positively associated with brain-age delta in females and, although WMH were positively associated with both CU females and males, only MCI males showed this positive association. Positive associations between NfL and WMH have been previously demonstrated, for both CU and MCI (Osborn et al., 2018), and the different AD stages (Walsh et al., 2021). Moreover, it has been proposed that WMH may reflect two different pathological pathways, one including amyloid aggregation and another including axonal injury (Osborn et al., 2018). Our results may suggest that brain aging in males might be driven more strongly by the former pathway, while brain aging in females might be driven more by the latter one.

Our purpose was to study the clinical validity of using the brain-age delta as a proxy biomarker of brain aging associated to AD and neurodegeneration. Therefore, our main aim was studying the characteristics of the individuals whose brain age is more accelerated or decelerated. One of the strengths of this study was the robustness of the brain-age delta measurement using a widely used segmentation atlas such as the Desikan-Killiany. Notably, we demonstrated the robustness of our method by training our model with one cohort and testing independently on four independent cohorts. The similar results obtained in all cohorts allowed us to seek associations in a large sample of participants with biomarker data and to further stratify the data by sex. This aspect is critical for this type of analyses as the effects of biological aging are necessarily very small, particularly in CU individuals of limited age range. This may explain why we could not detect significant effects versus longitudinal brain atrophy, as the available sample size for these analyses were smaller since this variable was not available in all cohorts. Another strength of our work was that we were able to include a wide range of different biomarkers of AD pathology allowing us to perform an in-depth analysis of the effect of these measurements with the brain-age delta. Conversely, our model used a smaller

number of features and a training set with a more limited age range than other models seen in literature recently (Liem et al., 2017; Peng et al., 2021), leading to a performance which cannot be compared against these state-of-the-art models. However, the performance of age prediction was similar to other publications that used similar methodologies (Beheshti et al., 2018; Dafflon et al., 2020; de Lange, et al., 2020) and, most importantly, was successful in studying the utility of brain-age delta as biomarker for AD and neurodegeneration. Future work should focus on developing a model with larger number of features or a 3D model and should study the effect of these validation measurements for AD and neurodegeneration with the brain-age delta more in depth.

In conclusion, we validated that machine-learning based brain age prediction obtained from a widely used segmentation atlas can be used as a biomarker of biological brain aging associated with AD pathology, risk factors and neurodegeneration. Moreover, our results confirm the presence of sex-related brain aging structural changes and suggest the prevalence of different neuropathological pathways involved in brain aging within females and males. Therefore, these results show the necessity to consider different approaches for assessing aging and neurodegeneration differently for each sex.

MATERIALS AND METHODS

Participants

We used a collection of T1-weighted brain MRI scans included in the UKBiobank (www.ukbiobank.ac.uk) dataset for training the proposed model and for calculating cross-validated brain age predictions. The dataset consisted of CU individuals (N = 22,661), after excluding subjects with ICD-9 and ICD-10 diagnosis, covering individuals of ages 44 to 81.

We also used four different cohorts to investigate the association between brain-age deltas with different sets of biomarker and AD risk factor measurements. Inclusion criteria for the independent cohorts consisted of: (i) availability of T1-weighted MRI brain scans; (ii) and availability of apolipoprotein E (*APOE*) categories and of CSF or PET measures for amyloid-β pathology acquired in less than a year from the MRI acquisition. These datasets included CU and MCI subjects from ADNI 1,2 and 3 (N = 751, CU = 253, MCI = 498), CU and MCI (as specified by a Clinical Dementia Rating = 0.5) subjects from the EPAD cohort (N = 808, CU = 653, MCI = 155), CU subjects from the ALFA+ cohort (N =380) and CU subjects from the OASIS cohort (N =407).

All the individuals had available data for the following clinical variables: chronological age, sex, MMSE and years of education, which will be referred as clinical variables from now on. A more detailed description of the clinical variables of these datasets is given in Table 1. Regarding AD-related variables, ALFA+, ADNI and EPAD cohorts included CSF $A\beta$42 measurements for categorizing $A\beta$ pathology status, AT status determined by CSF Aβ42 and CSF p-tau, *APOE* categories and WMH. OASIS, meanwhile, only had data available for Aβ PET and *APOE* categories. In addition, ALFA+ and ADNI included biomarkers of neurodegeneration such as CSF NfL, plasma NfL and cortical atrophy measured by longitudinal changes in the so-called aging signature (Bakkour et al., 2013). The combination of available AD-related variables and neurodegeneration biomarkers

will be referred as validation variables from so on. A more detailed description of the validation variables can be seen in Table 2.

Image Acquisition and Preprocessing

The UKBioBank, ADNI and OASIS datasets had available T1-weighted magnetic resonance (MR) images that had already been segmented with Freesurfer and had been parcellated using the FreeSurfer's cortical Desikan-Killiany(Desikan et al., 2006) and subcortical aseg(Fischl et al., 2002) labeling pipelines, which had undergone a quality control procedure. Taking advantage of this available data, we decided to use the same segmentation pipeline with the ALFA+ and EPAD cohorts. All the image acquisition and preprocessing done is as follows.

The UKBiobank dataset consisted of T1-weighted magnetic resonance (MR) images, all collected using a 3T Siemens Skyra scanner and preprocessed as previously explained in more detail (https://biobank.ctsu.ox.ac.uk/crystal/crystal/docs/brain_mri.pdf). Images were previously segmented with Freesurfer 6.0 and underwent a quality control procedure.

For ADNI participants (Petersen et al., 2010), MRI acquisition methods are described in more detail elsewhere (http:// adni.loni.usc.edu/methods/documents/). In brief, most of the T1-weighted MR were MP-RAGE, acquired with 1.5T or 3T scanners. Images were segmented with Freesurfer 5.1 and 6.0 and subjected to a quality control procedure. When possible, we also included a second T1-weighted MRI image sequence for the participants that underwent another MRI visit 3 years later. These scans were also segmented following the previously explained procedure.

For the OASIS subjects (Marcus et al., 2007), the MRI scans were acquired on 1.5 T or on 3.0 T scanners. T1-weighted magnetization-prepared rapid gradient echo (MP-RAGE) scans were obtained according to previously explained protocol (https://theunitedconsortium.com/wp-content/uploads/2021/07/OASIS-3_Imaging_Data_Dictionary_v1.8.pdf). All MRI sessions were segmented using FreeSurfer 5.1 or 5.3 and followed quality control measures. The PET images were acquired with [11C]PIB Pittsburgh's compound 60-minute dynamic PET scan in 3D mode and the corresponding analysis analyses were performed using the PET unified pipeline (PUP, https://github.com/ysu001/PUP). Mean standardized uptake value (SUVR) values were converted to Centiloid scale as previously explained.

For the ALFA+ participants, a high-resolution 3D T1-weighted MRI sequence was acquired in a 3T Philips Ingenia CX scanner (TE/TR=4.6/9.9 ms, Flip Angle = 8º; voxel size= 0.75x0.75x0.75 mm). Images were segmented with Freesurfer 6.0 and subjected to a quality control procedure to identify and remove incidental findings (Brugulat-Serrat et al., 2017) and segmentation errors(Huguet et al., 2021). Some of these ALFA+ subjects (N=187) underwent a second MRI visit 3 years after the initial visit, where another T1-weighted MRI sequence was acquired and segmented following the same procedure as in the first visit.

For the EPAD cohort(Solomon et al., 2018), which is a multisite study, T1-weighted MRIs were inversion-recovery prepare 3D gradient-echo sequences, acquired with 3T

scanners. Images were segmented with Freesurfer 6.0 and subjected to a quality control procedure (Lorenzini et al., 2021).

For all the cohorts, subsequent to the FreeSurfer segmentation, tissue regions were parcellated into 183 different anatomical regions of interest (ROI)s using the widely-used FreeSurfer's cortical Desikan-Killiany(Desikan et al., 2006) and subcortical aseg(Fischl et al., 2002) labeling pipelines. As mentioned before, we used the available FreeSurfer segmentations from UKBioBank, ADNI and OASIS cohorts. All volumes were residualized with respect to total intracranial volume (TIV) and to scanning site, while all cortical thicknesses were residualized with respect to scanning site, using linear models. Lastly, we performed a standardization procedure by computing z-score measurements feature-wise within each cohort, as previously performed (Casamitjana et al., 2018; Subramaniapillai et al., 2021; Ten Kate et al., 2018). We then assessed that there were not statistical differences in mean cortical thickness and volumes between the cohorts (see Supplementary Fig. 4).

Biomarkers

CSF and plasma collection, processing and biomarkers measurements

CSF and blood collection, processing and storage in the ALFA+ study have been described previously (Milà-Alomà et al., 2020a; Suárez-Calvet et al., 2020). CSF p-tau181 was measured using the Elecsys® Phospho-Tau (181P) CSF electrochemiluminescence immunoassay on a fully automated cobas e 601 instrument (Roche Diagnostics International Ltd, Rotkreuz, Switzerland). CSF Aβ42 and NfL were measured with the NeuroToolKit on a cobas e 411 or cobas e 601 instrument (Roche Diagnostics International Ltd, Rotkreuz, Switzerland). Plasma NfL was measured using the commercial Quanterix® assay (Simoa® NF-light Kit cat. no. 103186) on a HD-X analyzer following the manufacturer's instructions (Quanterix, Billerica, MA, USA). All these measurements were previously reported (Milà-Alomà et al., 2020; Suárez-Calvet et al., 2020). All measurements were performed at the Clinical Neurochemistry Laboratory, University of Gothenburg, Mölndal, Sweden, by laboratory technicians and scientists blinded to participants' clinical information.

In the ADNI study, CSF samples were measured according to the kit manufacturer's instructions and as described in previous studies (Bittner et al., 2016), using the Elecsys β-amyloid(1–42) CSF (Bittner et al., 2016) , and the Elecsys Phospho-Tau (181P) and Elecsys Total-Tau CSF immunoassays on a cobas e 601 analyzer at the Biomarker Research Laboratory, University of Pennsylvania, USA. Plasma NfL was measured on an in-house immunoassay on the single-molecule array (Simoa) platform, using the same methodology as described previously, at the Clinical Neurochemistry Laboratory, University of Gothenburg, Mölndal, Sweden.

In the EPAD study, CSF was measured using the Elecsys β-amyloid (1–42) and the Elecsys Phospho-Tau (181P) CSF electrochemiluminescence immunoassay on a fully automated cobas e 601 instrument (Roche Diagnostics International Ltd.). All measurements were performed at the Clinical Neurochemistry Laboratory, University of Gothenburg, Mölndal, Sweden, by laboratory technicians and scientists blinded to

participants' clinical information. Concentrations of CSF Aβ42 and p-tau181 were determined according to the manufacturer's instructions(Solomon et al., 2018).

Amyloid-β positivity cutoffs

For ALFA+, ADNI and EPAD, AT stages were defined by CSF Aβ42 and CSF p-tau, respectively. Previously used cut-offs were applied to each cohort, consisting of 1098 pg/mL for CSF Aβ42 for ALFA+ and EPAD (Schindler et al., 2018) and of 880 pg/mL for CSF Aβ42 for ADNI (Hansson et al., 2018) and of 24 pg/mL for p-tau for the three cohorts (Milà-Alomà et al., 2020). For OASIS, we used the cut-off value of 17 Centiloids from literature(Salvadó et al., 2019).

WMH Volumes

WMH volumes were generated for ALFA+ and EPAD cohorts using Bayesian Model Selection (BaMoS) procedure (Sudre et al., 2015), which has been provided previously. We also obtained the already available WMH volumes for ADNI cohort, in which the method of WMH volumetric quantification was performed using probabilistic models in a Markov Random Field framework, as previously provided (Schwarz et al., 2009). For each cohort, total WMH volumes were derived by summing and multiplying the number of labeled voxels by voxel dimensions. Total WMH volumes were natural log transformed and residualized with respect to TIV using linear models.

Aging signature measurements

For ALFA+ and ADNI, we computed the weighted Dickerson's aging signature (Bakkour et al., 2013), which has been used as a proxy measurement for brain aging. The aging signature is a map of specific brain regions that undergo cortical atrophy in normal aging. This meta-ROI is composed of the surface-area weighted average of the mean cortical thickness in the following individual ROIs: calcarine, caudal fusiform, caudal insula, cuneus, inferior frontal gyrus, medial superior frontal and precentral cortices. A Z-score of this aging-specific measure was calculated based on the mean and standard deviation of the CU individuals, as done previously (Bakkour et al., 2013). This is referred as Aging Signature V1.

In addition, we also computed this measurement on the scanners from the second MRI visit, referred as Aging Signature V2. We then computed a longitudinal brain atrophy measurement by computing the aging signature change over the years between the MRI acquisitions. Therefore, longitudinal aging signature change was computed as:

$$\text{Aging signature change} = \frac{\text{aging signature Visit 2} - \text{aging signature Visit 1}}{\text{Time between visits}}$$

For another secondary analysis shown in Supplementary Table 9, we also computed the aging signature (Aging Signature V1) for the remaining independent cohorts: EPAD and OASIS.

Brain-Age Prediction

Regression Model

Model Workflow

For the current study, we used a gradient boosting framework: the XGBoost regressor model from the XGBoost python package (https://xgboost.readthedocs.io/en/latest/python) to run the brain age prediction. This regressor, which is based on a decision-tree based ensemble algorithm, was selected due to its speed and performance and its advanced regularization to reduce overfitting (Chen & Guestrin, 2016)**.** In addition, large-scale brain age studies have demonstrated its adequacy (Bashyam et al., 2020; de Lange et al., 2019; de Lange, Barth, et al., 2020; Kaufmann et al., 2019). As it has been shown that there are sex-related trajectories in normal aging (Podgórski et al., 2021), we trained separate models for females and males. For each model, we first performed Bayesian parameter optimization based on a cross-validation scheme with ten folds and ten repeats per fold using the FreeSurfer volumes and thickness of the UK BioBank as input. For the optimization we used HYPEROPT (Bergstra et al., 2013), with which we scanned for maximum depth, number of estimators, learning rate, alpha regularization, lambda regularization, subsample, gamma and colsample by tree. The optimized parameters were maximum depth = 4, number of estimators = 800, learning rate = 0.03, alpha regularization = 4, lambda regularization =1, subsample= 0.36, gamma = 3 and colsample by tree = 0.89 for the males model; and maximum depth = 4, number of estimators = 850, learning rate = 0.03, alpha regularization = 8.5, lambda regularization =14.5, subsample= 0.449, gamma = 3.5 and colsample by tree = 0.72 for the females model. We trained these two models and performed the brain-age prediction on the independent cohorts. We decided to compute a ROI based model using these 183 FreeSurfer regions because they are widely used and available in most of the neuroimaging datasets. Therefore, our aim was not to compare our performance to the one achieved by a model trained with larger number of ROIs or with the full 3D images, but to study the generalizability and the relevance of our model in the AD field.

Contribution of Brain Regions in prediction

We computed SHAP (SHapley Additive exPlanation) values (https://github.com/slundberg/shap) to measure the contribution of each brain region in the prediction of age for each subject. SHAP assigns an importance value within the prediction to each feature (in this case, brain region), which is based on its unique consistent and locally accurate attribution (Lundberg et al., 2020). We calculated the average SHAP value for each region for all females and males of the UK BioBank cohort.

In addition, to assess that the regions with highest SHAP values were stable, we performed a permutation approach to study the significance of each region, separately for females and males. With this aim we compared the averaged SHAP value (region-specific) obtained when using the entire train set on the model to a null distribution calculated from 1,000 permutations performing subsample of the subjects, in which we trained and tested the model using 80% and 20% of the individuals, respectively.

Brain-Age Delta Estimation

We predicted brain-age on the independent cohorts separately: ALFA+, EPAD, ADNI and OASIS, using the previously trained model. To investigate the prediction performance, correlation analyses were run for predicted brain-age versus chronological age, R^2, root mean square error (RMSE), and mean absolute error (MAE) were calculated for each independent cohort separately, as well as for females and males separate pooled from all independent cohorts. We also investigated the prediction performance on the UKBioBank cohort by computing the average latter metrics from a cross validation with ten splits and ten repetitions.

As recent research has shown that brain-age estimation involves a proportional bias (de Lange & Cole, 2020; Le et al., 2018; Liang et al., 2019; Smith et al., 2019), we applied a well-established age-bias correction procedure to our data (de Lange & Cole, 2020; Le et al., 2018). This correction, as originally proposed (de Lange & Cole, 2020; Le et al., 2018), consists of a linear regression between age (Ω) and brain-predicted age (Y) on each of the independent cohorts, $Y = \alpha \times \Omega + \beta$. The derived values of slope (α) and intercept (β) from the training set were used to correct the predicted brain-age in each test set by applying: $\text{Corrected Predicted Brain Age} = \text{Predicted Brain Age} + [\Omega - (\alpha \times \Omega + \beta)]$. By subtracting the chronological age from the Corrected Predicted Brain Age, we obtained the brain-age delta which was used to test the associations with the validation measurements. The result of the correction is shown in Supplementary Fig.3.

Statistical Analyses

All statistical analyses were conducted using Python 3.7.0. We tested for normality of the distribution for each biomarker using the Kolmogorov-Smirnov test and visual inspection of histograms. CSF NfL and plasma NfL did not follow a normal distribution and were thus natural log transformed. In addition, to compare the measurements for CSF NfL and for plasma NfL coming from different cohorts (ALFA+ and ADNI), CSF and plasma NfL was converted to z-scores.

To study the performance and accuracy of the brain-age prediction for each cohort, correlation analyses were run for predicted brain-age versus chronological age. We also computed R^2, RMSE and MAE for each cohort, as well as the age bias of the prediction after bias correction. We assessed statistically whether the accuracy of the predicted brain-age was different between cohorts by using Fisher's z-transformation for correlation coefficients. In addition, we computed these performance metrics to assess the differences in the model for females and males in the pooled cohorts. Results from another secondary analysis are also shown in Supplementary Table 2, in which we assessed the performance and accuracy of the aging signature for all cohorts, by performing correlation analyses between the aging signature versus chronological age and computing the R^2 and RMSE. In this secondary analyses, we also studied whether the performance obtained for the predicted brain-age was better than the aging signature by performing the William's test (Williams, 1959) for the Pearson's correlation coefficient and a F-test to assess which model was statistically better.

We used the brain-age delta as a measure of brain aging to study the associations between this measurement and the different AD and neurodegeneration biomarkers and risk factors. With this aim, we pooled all the subjects from all cohorts together and computed linear regression models for each validation variable, in which chronological age and sex were included as covariates. Local effect size of each of the continuous validation

variables was calculated using Cohen's f^2 (Cohen, 2013). The mean brain age delta among Aβ pathology, AT stages and *APOE* status, were assessed by a one-way analysis of covariance (ANCOVA) adjusting for age and sex. Effect size of the different levels was calculated by dividing the estimated difference in the brain-age delta between the different categories by the estimated standard deviation. We also stratified the individuals by sex and studied the associations between brain-age delta and the different validation variables by computing linear regression models in which chronological age was included as covariate. We next tested for interactions between sex and the validation variables on brain-age delta using linear regression models and including chronological age as covariate. Lastly, we tested for interactions between age and the validation variables on brain-age delta for CU and MCI individuals.

We also studied the differences in volumes and cortical thickness between females and males in the UKBioBank for the brain regions that contributed the most to the prediction according to the SHAP values. With this aim we performed regression models for each ROI with sex as predictor variable, in which linear and quadratic expansions of age, site and TIV (only included for volume ROIs), were included as covariates.

As a secondary analysis we wanted to identify the individuals whose predicted brain-age deviate the most from chronological aging, i.e., individuals with the highest positive or lowest negative brain-age deltas, to study the above-mentioned associations. With this aim, we selected the individuals whose brain-age delta was included within the 10th and 90th percentile of the distribution for each independent cohort and studied the differences between these groups. The methodology and the results of this analysis can be found in Supplementary Appendix A.

ACKNOWLEDGEMENTS & FUNDING

This publication is part of the ALFA study (ALzheimer and FAmilies). The authors would like to express their most sincere gratitude to the ALFA project participants, without whom this research would have not been possible. Authors would like to thank Roche Diagnostics International Ltd. for kindly providing the kits for the CSF analysis of ALFA+ participants and GE Healthcare for kindly providing [18F]flutemetamol doses of ALFA+ participants. Collaborators of the ALFA Study are: Müge Akinci, Annabella Beteta, Alba Cañas, Irene Cumplido, Carme Deulofeu, Ruth Dominguez, Maria Emilio, Karine Fauria, Sherezade Fuentes, Oriol Grau-Rivera, Laura Hernandez, Gema Huesa, Jordi Huguet, Eider M Arenaza-Urquijo, Eva M Palacios, Paula Marne, Tania Menchón, Carolina Minguillon, Eleni Palpatzis, Cleofé Peña-Gómez, Albina Polo, Sandra Pradas, Blanca Rodríguez-Fernández, Aleix Sala-Vila, Gemma Salvadó, Mahnaz Shekari, Anna Soteras, Laura Stankeviciute, Marc Vilanova and Natalia Vilor-Tejedor.

The project leading to these results has received funding from "la Caixa" Foundation (ID 100010434), under agreement LCF/PR/GN17/50300004 and the Alzheimer's Association and an international anonymous charity foundation through the TriBEKa Imaging Platform project (TriBEKa-17-519007). Additional support has been received from the Universities and Research Secretariat, Ministry of Business and Knowledge of the Catalan Government under the grant no. 2017-SGR-892 and the Spanish Research Agency (AEI) under project PID2020-116907RB-I00 of the call MCIN/ AEI

/10.13039/501100011033. FB is supported by the NIHR biomedical research center at UCLH. MSC receives funding from the European Research Council (ERC) under the European Union's Horizon 2020 research and innovation programme (Grant agreement No. 948677), the Instituto de Salud Carlos III (PI19/00155), and from a fellowship from "la Caixa" Foundation (ID 100010434) and from the European Union's Horizon 2020 research and innovation programme under the Marie Skłodowska-Curie grant agreement No 847648 (LCF/BQ/PR21/11840004).

COBAS, COBAS E and ELECSYS are trademarks of Roche. All other product names and trademarks are the property of their respective owners. The Roche NeuroToolKit is a panel of exploratory prototype assays designed to robustly evaluate biomarkers associated with key pathologic events characteristic of AD and other neurological disorders, used for research purposes only and not approved for clinical use.

CONFLICTS OF INTEREST

Ivonne Suridjan is a full-time employee and shareholder of Roche Diagnostics International Ltd; Gwendlyn Kollmorgen is a full-time employee of Roche Diagnostics GmbH; Anna Bayfield is a full-time employee and shareholder of Roche Diagnostics GmbH.

MSC has served as a consultant and at advisory boards for Roche Diagnostics International Ltd and has given lectures in symposia sponsored by Roche Diagnostics, S.L.U, Roche Farma, S.A and Roche Sistemas de Diagnósticos, Sociedade Unipessoal, Lda.

JL.M is currently a full-time employee of H. Lundbeck A/S and previously has served as a consultant or on advisory boards for the following for-profit companies or has given lectures in symposia sponsored by the following for-profit companies: Roche Diagnostics, Genentech, Novartis, Lundbeck, Oryzon, Biogen, Lilly, Janssen, Green Valley, MSD, Eisai, Alector, BioCross, GE Healthcare, and ProMIS Neurosciences.

REFERENCES

Arenaza-Urquijo, E. M., Przybelski, S. A., Lesnick, T. L., Graff-Radford, J., Machulda, M. M., Knopman, D. S., Schwarz, C. G., Lowe, V. J., Mielke, M. M., Petersen, R. C., Jack, C. R., Jr., & Vemuri, P. (2019). The metabolic brain signature of cognitive resilience in the 80+: beyond Alzheimer pathologies. *Brain*, *142*(4), 1134. https://doi.org/10.1093/BRAIN/AWZ037

Armstrong, N. M., An, Y., Beason-Held, L., Doshi, J., Erus, G., Ferrucci, L., Davatzikos, C., & Resnick, S. M. (2019). Sex differences in brain aging and predictors of neurodegeneration in cognitively healthy older adults. *Neurobiology of Aging*, *81*, 146–156. https://doi.org/10.1016/J.NEUROBIOLAGING.2019.05.020

Bakkour, A., Morris, J. C., Wolk, D. A., & Dickerson, B. C. (2013). The effects of aging and

Alzheimer's disease on cerebral cortical anatomy: Specificity and differential relationships with cognition. *NeuroImage*, *76*, 332–344. https://doi.org/10.1016/j.neuroimage.2013.02.059

Baron-Cohen, S., Knickmeyer, R. C., & Belmonte, M. K. (2005). Sex differences in the brain: Implications for explaining autism. *Science*, *310*(5749), 819–823. https://doi.org/10.1126/SCIENCE.1115455

Bashyam, V. M., Erus, G., Doshi, J., Habes, M., Nasralah, I., Truelove-Hill, M., Srinivasan, D., Mamourian, L., Pomponio, R., Fan, Y., Launer, L. J., Masters, C. L., Maruff, P., Zhuo, C., Völzke, H., Johnson, S. C., Fripp, J., Koutsouleris, N., Satterthwaite, T. D., … Davatzikos, C. (2020). MRI signatures of brain age and disease over the lifespan based on a deep brain network and 14 468 individuals worldwide. *Brain : A Journal of Neurology*, *143*(7), 2312–2324. https://doi.org/10.1093/brain/awaa160

Beheshti, I., Maikusa, N., & Matsuda, H. (2018). The association between "Brain-Age Score" (BAS) and traditional neuropsychological screening tools in Alzheimer's disease. *Brain and Behavior*, *8*(8), e01020. https://doi.org/10.1002/brb3.1020

Bergstra, J., Yamins, D., & Cox, D. D. (2013). Making a Science of Model Search: Hyperparameter Optimization in Hundreds of Dimensions for Vision Architectures. *Proc. of the 30th International Conference on Machine Learning (ICML 2013)*, *28*, I-115 to I–23.

Bittner, T., Zetterberg, H., Teunissen, C. E., Ostlund, R. E., Militello, M., Andreasson, U., Hubeek, I., Gibson, D., Chu, D. C., Eichenlaub, U., Heiss, P., Kobold, U., Leinenbach, A., Madin, K., Manuilova, E., Rabe, C., & Blennow, K. (2016). Technical performance of a novel, fully automated electrochemiluminescence immunoassay for the quantitation of β-amyloid (1-42) in human cerebrospinal fluid. *Alzheimer's and Dementia*, *12*(5), 517–526. https://doi.org/10.1016/j.jalz.2015.09.009

Brugulat-Serrat, A., Rojas, S., Bargalló, N., Conesa, G., Minguillón, C., Fauria, K., Gramunt, N., Molinuevo, J. L., & Gispert, J. D. (2017). Incidental findings on brain MRI of cognitively normal first-degree descendants of patients with Alzheimer's disease: a cross-sectional analysis from the ALFA (Alzheimer and Families) project. *BMJ Open*, *7*(3). https://doi.org/10.1136/BMJOPEN-2016-013215

Brugulat-Serrat, A., Salvadó, G., Operto, G., Cacciaglia, R., Sudre, C. H., Grau-Rivera, O., Suárez-Calvet, M., Falcon, C., Sánchez-Benavides, G., Gramunt, N., Minguillon, C., Fauria, K., Barkhof, F., Molinuevo, J. L., & Gispert, J. D. (2020). White matter hyperintensities mediate gray matter volume and processing speed relationship in cognitively unimpaired participants. *Human Brain Mapping*, *41*(5), 1309–1322. https://doi.org/10.1002/hbm.24877

Brugulat-Serrat, A., Salvadó, G., Sudre, C. H., Grau-Rivera, O., Suárez-Calvet, M., Falcon, C., Sánchez-Benavides, G., Gramunt, N., Fauria, K., Cardoso, M. J., Barkhof, F., Molinuevo, J. L., Gispert, J. D., Camí, J., Cacciaglia, R., Operto, G., Skouras, S., Minguillón, C., Polo, A., … Huguet, J. (2020). Patterns of white matter hyperintensities associated with cognition in middle-aged cognitively healthy individuals. *Brain Imaging and Behavior*, *14*(5), 2012–2023. https://doi.org/10.1007/s11682-019-00151-2

Buckley, R. F., Mormino, E. C., Rabin, J. S., Hohman, T. J., Landau, S., Hanseeuw, B. J., Jacobs, H. I. L., Papp, K. V., Amariglio, R. E., Properzi, M. J., Schultz, A. P., Kirn, D., Scott, M. R., Hedden, T., Farrell, M., Price, J., Chhatwal, J., Rentz, D. M., Villemagne, V. L., … Sperling, R. A. (2019). Sex Differences in the Association of Global Amyloid and Regional Tau Deposition Measured by Positron Emission Tomography in Clinically Normal Older Adults. *JAMA Neurology*, *76*(5), 542–551. https://doi.org/10.1001/jamaneurol.2018.4693

Casamitjana, A., Petrone, P., Tucholka, A., Falcon, C., Skouras, S., Molinuevo, J. L., Vilaplana, V., & Gispert, J. D. (2018). MRI-Based Screening of Preclinical Alzheimer's Disease for Prevention Clinical Trials. *Journal of Alzheimer's Disease : JAD*, *64*(4), 1099–1112. https://doi.org/10.3233/JAD-180299

Chen, T., & Guestrin, C. (2016). XGBoost: A scalable tree boosting system. *Proceedings of the 22nd ACM SIGKDD International Conference on Knowledge Discovery and Data Mining*, 785–794. https://doi.org/10.1145/2939672.2939785

Coffey, C. E., Lucke, J. F., Saxton, J. A., Ratcliff, G., Unitas, L. J., Billig, B., & Bryan, R. N. (1998). Sex differences in brain aging: A quantitative magnetic resonance imaging study. *Archives of Neurology*, *55*(2), 169–179. https://doi.org/10.1001/archneur.55.2.169

Cohen, J. (2013). Statistical Power Analysis for the Behavioral Sciences. In Lawrence Erlbaum Associates Inc (Ed.), *Statistical Power Analysis for the Behavioral Sciences*. Routledge. https://doi.org/10.4324/9780203771587

Cole, J. H., Ritchie, S. J., Bastin, M. E., Valdés Hernández, M. C., Muñoz Maniega, S., Royle, N., Corley, J., Pattie, A., Harris, S. E., Zhang, Q., Wray, N. R., Redmond, P., Marioni, R. E., Starr, J. M., Cox, S. R., Wardlaw, J. M., Sharp, D. J., & Deary, I. J. (2018). Brain age predicts mortality. *Molecular Psychiatry*, *23*(5), 1385–1392. https://doi.org/10.1038/mp.2017.62

Cole, James H. (2020). Multimodality neuroimaging brain-age in UK biobank: relationship to biomedical, lifestyle, and cognitive factors. *Neurobiology of Aging*, *92*, 34–42. https://doi.org/10.1016/j.neurobiolaging.2020.03.014

Cole, James H., & Franke, K. (2017). Predicting Age Using Neuroimaging: Innovative Brain Ageing Biomarkers. *Trends in Neurosciences*, *40*(12), 681–690. https://doi.org/10.1016/J.TINS.2017.10.001

Cole, James H., Poudel, R. P. K., Tsagkrasoulis, D., Caan, M. W. A., Steves, C., Spector, T. D., & Montana, G. (2017). Predicting brain age with deep learning from raw imaging data results in a reliable and heritable biomarker. *NeuroImage*, *163*, 115–124. https://doi.org/10.1016/J.NEUROIMAGE.2017.07.059

Dafflon, J., Pinaya, W. H. L., Turkheimer, F., Cole, J. H., Leech, R., Harris, M. A., Cox, S. R., Whalley, H. C., McIntosh, A. M., & Hellyer, P. J. (2020). An automated machine learning approach to predict brain age from cortical anatomical measures. *Human Brain Mapping*, *41*(13), 3555–3566. https://doi.org/10.1002/hbm.25028

de Lange, A. M. G., Anatürk, M., Suri, S., Kaufmann, T., Cole, J. H., Griffanti, L., Zsoldos, E., Jensen, D. E. A., Filippini, N., Singh-Manoux, A., Kivimäki, M., Westlye, L. T., &

Ebmeier, K. P. (2020). Multimodal brain-age prediction and cardiovascular risk: The Whitehall II MRI sub-study. *NeuroImage*, *222*, 117292. https://doi.org/10.1016/j.neuroimage.2020.117292

de Lange, A. M. G., Barth, C., Kaufmann, T., Maximov, I. I., van der Meer, D., Agartz, I., & Westlye, L. T. (2020). Women's brain aging: Effects of sex-hormone exposure, pregnancies, and genetic risk for Alzheimer's disease. *Human Brain Mapping*, *41*(18), 5141–5150. https://doi.org/10.1002/hbm.25180

de Lange, A. M. G., & Cole, J. H. (2020). Commentary: Correction procedures in brain-age prediction. In *NeuroImage: Clinical* (Vol. 26). Elsevier Inc. https://doi.org/10.1016/j.nicl.2020.102229

de Lange, A. M. G., Kaufmann, T., Van Der Meer, D., Maglanoc, L. A., Alnæs, D., Moberget, T., Douaud, G., Andreassen, O. A., & Westlye, L. T. (2019). Population-based neuroimaging reveals traces of childbirth in the maternal brain. *Proceedings of the National Academy of Sciences of the United States of America*, *116*(44), 22341–22346. https://doi.org/10.1073/pnas.1910666116

DeCarli, C., Massaro, J., Harvey, D., Hald, J., Tullberg, M., Au, R., Beiser, A., D'Agostino, R., & Wolf, P. A. (2005). Measures of brain morphology and infarction in the framingham heart study: establishing what is normal. *Neurobiology of Aging*, *26*(4), 491–510. https://doi.org/10.1016/J.NEUROBIOLAGING.2004.05.004

Desikan, R. S., Ségonne, F., Fischl, B., Quinn, B. T., Dickerson, B. C., Blacker, D., Buckner, R. L., Dale, A. M., Maguire, R. P., Hyman, B. T., Albert, M. S., & Killiany, R. J. (2006). An automated labeling system for subdividing the human cerebral cortex on MRI scans into gyral based regions of interest. *NeuroImage*, *31*(3), 968–980. https://doi.org/10.1016/j.neuroimage.2006.01.021

Evans, S., Dowell, N. G., Tabet, N., Tofts, P. S., King, S. L., & Rusted, J. M. (2014). Cognitive and neural signatures of the APOE E4 allele in mid-aged adults. *Neurobiology of Aging*, *35*(7), 1615–1623. https://doi.org/10.1016/J.NEUROBIOLAGING.2014.01.145

Ferretti, M. T., Iulita, M. F., Cavedo, E., Chiesa, P. A., Dimech, A. S., Chadha, A. S., Baracchi, F., Girouard, H., Misoch, S., Giacobini, E., Depypere, H., & Hampel, H. (2018). Sex differences in Alzheimer disease — The gateway to precision medicine. In *Nature Reviews Neurology* (Vol. 14, Issue 8, pp. 457–469). Nature Publishing Group. https://doi.org/10.1038/s41582-018-0032-9

Filippini, N., Ebmeier, K. P., MacIntosh, B. J., Trachtenberg, A. J., Frisoni, G. B., Wilcock, G. K., Beckmann, C. F., Smith, S. M., Matthews, P. M., & Mackay, C. E. (2011). Differential effects of the APOE genotype on brain function across the lifespan. *NeuroImage*, *54*(1), 602–610. https://doi.org/10.1016/J.NEUROIMAGE.2010.08.009

Fischl, B., Salat, D. H., Busa, E., Albert, M., Dieterich, M., Haselgrove, C., Van Der Kouwe, A., Killiany, R., Kennedy, D., Klaveness, S., Montillo, A., Makris, N., Rosen, B., & Dale, A. M. (2002). Whole brain segmentation: Automated labeling of neuroanatomical structures in the human brain. *Neuron*, *33*(3), 341–355. https://doi.org/10.1016/S0896-6273(02)00569-X

669 Fjell, A. M., McEvoy, L., Holland, D., Dale, A. M., & Walhovd, K. B. (2014). What is normal
670 in normal aging? Effects of aging, amyloid and Alzheimer's disease on the cerebral cortex
671 and the hippocampus. In *Progress in Neurobiology* (Vol. 117, pp. 20–40). Elsevier Ltd.
672 https://doi.org/10.1016/j.pneurobio.2014.02.004

673 Franke, K., & Gaser, C. (2019). Ten years of brainage as a neuroimaging biomarker of brain
674 aging: What insights have we gained? *Frontiers in Neurology*, *10*, 789.
675 https://doi.org/10.3389/fneur.2019.00789

676 Franke, K., Ziegler, G., Klöppel, S., & Gaser, C. (2010). Estimating the age of healthy subjects
677 from T1-weighted MRI scans using kernel methods: Exploring the influence of various
678 parameters. *NeuroImage*, *50*(3), 883–892.
679 https://doi.org/10.1016/J.NEUROIMAGE.2010.01.005

680 Gennatas, E. D., Avants, B. B., Wolf, D. H., Satterthwaite, T. D., Ruparel, K., Ciric, R.,
681 Hakonarson, H., Gur, R. E., & Gur, R. C. (2017). Age-Related Effects and Sex
682 Differences in Gray Matter Density, Volume, Mass, and Cortical Thickness from
683 Childhood to Young Adulthood. *The Journal of Neuroscience*, *37*(20), 5065.
684 https://doi.org/10.1523/JNEUROSCI.3550-16.2017

685 Green, P. S., & Simpkins, J. W. (2000). Neuroprotective effects of estrogens: Potential
686 mechanisms of action. In *International Journal of Developmental Neuroscience* (Vol. 18,
687 Issues 4–5, pp. 347–358). John Wiley & Sons, Ltd. https://doi.org/10.1016/S0736-
688 5748(00)00017-4

689 Greenberg, D. L., Messer, D. F., Payne, M. E., MacFall, J. R., Provenzale, J. M., Steffens, D.
690 C., & Krishnan, R. R. (2008). Aging, gender, and the elderly adult brain: An examination
691 of analytical strategies. *Neurobiology of Aging*, *29*(2), 290–302.
692 https://doi.org/10.1016/j.neurobiolaging.2006.09.016

693 Habes, M., Erus, G., Toledo, J. B., Zhang, T., Bryan, N., Launer, L. J., Rosseel, Y., Janowitz,
694 D., Doshi, J., Van Der Auwera, S., Von Sarnowski, B., Hegenscheid, K., Hosten, N.,
695 Homuth, G., Völzke, H., Schminke, U., Hoffmann, W., Grabe, H. J., & Davatzikos, C.
696 (2016). White matter hyperintensities and imaging patterns of brain ageing in the general
697 population. *Brain*, *139*(4), 1164. https://doi.org/10.1093/BRAIN/AWW008

698 Hansson, O., Seibyl, J., Stomrud, E., Zetterberg, H., Trojanowski, J. Q., Bittner, T., Lifke, V.,
699 Corradini, V., Eichenlaub, U., Batrla, R., Buck, K., Zink, K., Rabe, C., Blennow, K., &
700 Shaw, L. M. (2018). CSF biomarkers of Alzheimer's disease concord with amyloid-β PET
701 and predict clinical progression: A study of fully automated immunoassays in BioFINDER
702 and ADNI cohorts. *Alzheimer's and Dementia*, *14*(11), 1470–1481.
703 https://doi.org/10.1016/j.jalz.2018.01.010

704 Huang, W., Li, X., Li, H., Wang, W., Chen, K., Xu, K., Zhang, J., Chen, Y., Wei, D., Shu, N.,
705 & Zhang, Z. (2021). Accelerated Brain Aging in Amnestic Mild Cognitive Impairment:
706 Relationships with Individual Cognitive Decline, Risk Factors for Alzheimer Disease and
707 Clinical Progression. *Radiology: Artificial Intelligence*, e200171.
708 https://doi.org/10.1148/ryai.2021200171

709 Huguet, J., Falcon, C., Fusté, D., Girona, S., Vicente, D., Molinuevo, J. L., Gispert, J. D.,
710 Operto, G., & Study, for the A. (2021). Management and Quality Control of Large

Neuroimaging Datasets: Developments From the Barcelonaβeta Brain Research Center. *Frontiers in Neuroscience*, *15*. https://doi.org/10.3389/FNINS.2021.633438

Jack, C. R., Bennett, D. A., Blennow, K., Carrillo, M. C., Dunn, B., Haeberlein, S. B., Holtzman, D. M., Jagust, W., Jessen, F., Karlawish, J., Liu, E., Molinuevo, J. L., Montine, T., Phelps, C., Rankin, K. P., Rowe, C. C., Scheltens, P., Siemers, E., Snyder, H. M., … Silverberg, N. (2018). NIA-AA Research Framework: Toward a biological definition of Alzheimer's disease. *Alzheimer's and Dementia*, *14*(4), 535–562. https://doi.org/10.1016/j.jalz.2018.02.018

Kaeser, S. A., Lehallier, B., Thinggaard, M., Häsler, L. M., Apel, A., Bergmann, C., Berdnik, D., Jeune, B., Christensen, K., Grönke, S., Partridge, L., Wyss-Coray, T., Mengel-From, J., & Jucker, M. (2021). A neuronal blood marker is associated with mortality in old age. *Nature Aging*, *1*(2), 218–225. https://doi.org/10.1038/s43587-021-00028-4

Kaufmann, T., van der Meer, D., Doan, N. T., Schwarz, E., Lund, M. J., Agartz, I., Alnæs, D., Barch, D. M., Baur-Streubel, R., Bertolino, A., Bettella, F., Beyer, M. K., Bøen, E., Borgwardt, S., Brandt, C. L., Buitelaar, J., Celius, E. G., Cervenka, S., Conzelmann, A., … Westlye, L. T. (2019). Common brain disorders are associated with heritable patterns of apparent aging of the brain. *Nature Neuroscience*, *22*(10), 1617–1623. https://doi.org/10.1038/s41593-019-0471-7

Khalil, M., Pirpamer, L., Hofer, E., Voortman, M. M., Barro, C., Leppert, D., Benkert, P., Ropele, S., Enzinger, C., Fazekas, F., Schmidt, R., & Kuhle, J. (2020). Serum neurofilament light levels in normal aging and their association with morphologic brain changes. *Nature Communications*, *11*(1), 1–9. https://doi.org/10.1038/s41467-020-14612-6

Khalil, M., Teunissen, C. E., Otto, M., Piehl, F., Sormani, M. P., Gattringer, T., Barro, C., Kappos, L., Comabella, M., Fazekas, F., Petzold, A., Blennow, K., Zetterberg, H., & Kuhle, J. (2018). Neurofilaments as biomarkers in neurological disorders. *Nature Reviews Neurology*, *14*(10), 577–589. https://doi.org/10.1038/s41582-018-0058-z

Le, T. T., Kuplicki, R. T., McKinney, B. A., Yeh, H. W., Thompson, W. K., Paulus, M. P., Aupperle, R. L., Bodurka, J., Cha, Y. H., Feinstein, J. S., Khalsa, S. S., Savitz, J., Simmons, W. K., & Victor, T. A. (2018). A Nonlinear Simulation Framework Supports Adjusting for Age When Analyzing BrainAGE. *Frontiers in Aging Neuroscience*, *10*, 317. https://doi.org/10.3389/fnagi.2018.00317

Liang, H., Zhang, F., & Niu, X. (2019). Investigating systematic bias in brain age estimation with application to post-traumatic stress disorders. *Human Brain Mapping*, *40*(11), 3143–3152. https://doi.org/10.1002/hbm.24588

Liem, F., Varoquaux, G., Kynast, J., Beyer, F., Kharabian Masouleh, S., Huntenburg, J. M., Lampe, L., Rahim, M., Abraham, A., Craddock, R. C., Riedel-Heller, S., Luck, T., Loeffler, M., Schroeter, M. L., Witte, A. V., Villringer, A., & Margulies, D. S. (2017). Predicting brain-age from multimodal imaging data captures cognitive impairment. *NeuroImage*, *148*, 179–188. https://doi.org/10.1016/J.NEUROIMAGE.2016.11.005

Lorenzini, L., Ingala, S., Wink, A. M., Kuijer, J. P., Wottschel, V., Dijsselhof, M., Sudre, C. H., Haller, S., Molinuevo, J. L., Gispert, J. D., Cash, D. M., Thomas, D. L., Vos, S. B.,

753 Prados, F., Petr, J., Wolz, R., Palombit, A., Schwarz, A. J., Gael, C., … for the EPAD
754 Consortium. (2021). The European Prevention of Alzheimer's Dementia (EPAD) MRI
755 Dataset and Processing Workflow. *BioRxiv*, 2021.09.29.462349.
756 https://doi.org/10.1101/2021.09.29.462349

757 Löwe, L. C., Gaser, C., Franke, K., & for the Alzheimer's Disease Neuroimaging Initiative.
758 (2016). The Effect of the APOE Genotype on Individual BrainAGE in Normal Aging,
759 Mild Cognitive Impairment, and Alzheimer's Disease. *PLoS ONE*, *11*(7).
760 https://doi.org/10.1371/JOURNAL.PONE.0157514

761 Lundberg, S. M., Erion, G., Chen, H., DeGrave, A., Prutkin, J. M., Nair, B., Katz, R.,
762 Himmelfarb, J., Bansal, N., & Lee, S.-I. (2020). From local explanations to global
763 understanding with explainable AI for trees. *Nature Machine Intelligence*, *2*(1), 56–67.
764 https://doi.org/10.1038/s42256-019-0138-9

765 Ly, M., Yu, G. Z., Karim, H. T., Muppidi, N. R., Mizuno, A., Klunk, W. E., & Aizenstein, H. J.
766 (2020). Improving brain age prediction models: incorporation of amyloid status in
767 Alzheimer's disease. *Neurobiology of Aging*, *87*, 44–48.
768 https://doi.org/10.1016/j.neurobiolaging.2019.11.005

769 Maioli, S., Leander, K., Nilsson, P., & Nalvarte, I. (2021). Estrogen receptors and the aging
770 brain. In *Essays in Biochemistry* (Vol. 65, Issue 6, pp. 913–925). Portland Press Ltd.
771 https://doi.org/10.1042/EBC20200162

772 Maniega, S. M., Valdés Hernández, M. C., Clayden, J. D., Royle, N. A., Murray, C., Morris, Z.,
773 Aribisala, B. S., Gow, A. J., Starr, J. M., Bastin, M. E., Deary, I. J., & Wardlaw, J. M.
774 (2015). White matter hyperintensities and normal-appearing white matter integrity in the
775 aging brain. *Neurobiology of Aging*, *36*(2), 909–918.
776 https://doi.org/10.1016/j.neurobiolaging.2014.07.048

777 Marcus, D. S., Wang, T. H., Parker, J., Csernansky, J. G., Morris, J. C., & Buckner, R. L.
778 (2007). Open Access Series of Imaging Studies (OASIS): Cross-sectional MRI data in
779 young, middle aged, nondemented, and demented older adults. *Journal of Cognitive*
780 *Neuroscience*, *19*(9), 1498–1507. https://doi.org/10.1162/jocn.2007.19.9.1498

781 Mielke, M. M. (2020). Consideration of Sex Differences in the Measurement and Interpretation
782 of Alzheimer Disease-Related Biofluid-Based Biomarkers. In *The journal of applied*
783 *laboratory medicine* (Vol. 5, Issue 1, pp. 158–169). NIH Public Access.
784 https://doi.org/10.1373/jalm.2019.030023

785 Milà-Alomà, M., Salvadó, G., Gispert, J. D., Vilor-Tejedor, N., Grau-Rivera, O., Sala-Vila, A.,
786 Sánchez-Benavides, G., Arenaza-Urquijo, E. M., Crous-Bou, M., González-de-Echávarri,
787 J. M., Minguillon, C., Fauria, K., Simon, M., Kollmorgen, G., Zetterberg, H., Blennow,
788 K., Suárez-Calvet, M., & Molinuevo, J. L. (2020). Amyloid beta, tau, synaptic,
789 neurodegeneration, and glial biomarkers in the preclinical stage of the Alzheimer's
790 continuum. *Alzheimer's and Dementia*, *16*(10), 1358–1371.
791 https://doi.org/10.1002/alz.12131

792 Nebel, R. A., Aggarwal, N. T., Barnes, L. L., Gallagher, A., Goldstein, J. M., Kantarci, K.,
793 Mallampalli, M. P., Mormino, E. C., Scott, L., Yu, W. H., Maki, P. M., & Mielke, M. M.
794 (2018). Understanding the impact of sex and gender in Alzheimer's disease: A call to

action. *Alzheimer's & Dementia*, *14*(9), 1171–1183. https://doi.org/10.1016/J.JALZ.2018.04.008

Osborn, K. E., Liu, D., Samuels, L. R., Moore, E. E., Cambronero, F. E., Acosta, L. M. Y., Bell, S. P., Babicz, M. A., Gordon, E. A., Pechman, K. R., Davis, L. T., Gifford, K. A., Hohman, T. J., Blennow, K., Zetterberg, H., & Jefferson, A. L. (2018). Cerebrospinal fluid β-amyloid42 and neurofilament light relate to white matter hyperintensities. *Neurobiology of Aging*, *68*, 18–25. https://doi.org/10.1016/j.neurobiolaging.2018.03.028

Peng, H., Gong, W., Beckmann, C. F., Vedaldi, A., & Smith, S. M. (2021). Accurate brain age prediction with lightweight deep neural networks. *Medical Image Analysis*, *68*, 101871. https://doi.org/10.1016/J.MEDIA.2020.101871

Petersen, R. C., Aisen, P. S., Beckett, L. A., Donohue, M. C., Gamst, A. C., Harvey, D. J., Jack, C. R., Jr, Jagust, W. J., Shaw, L. M., Toga, A. W., Trojanowski, J. Q., & Weiner, M. W. (2010). Alzheimer's Disease Neuroimaging Initiative (ADNI): Clinical characterization. *Neurology*, *74*(3), 201. https://doi.org/10.1212/WNL.0B013E3181CB3E25

Pichet Binette, A., Gonneaud, J., Vogel, J. W., La Joie, R., Rosa-Neto, P., Collins, D. L., Poirier, J., Breitner, J. C. S., Villeneuve, S., Vachon-Presseau, E., for the Alzheimer's Disease Neuroimaging, & the PREVENT-AD Research Group. (2020). Morphometric network differences in ageing versus Alzheimer's disease dementia. *Brain*, *143*(2), 635–649. https://doi.org/10.1093/BRAIN/AWZ414

Podgórski, P., Bladowska, J., Sasiadek, M., & Zimny, A. (2021). Novel Volumetric and Surface-Based Magnetic Resonance Indices of the Aging Brain – Does Male and Female Brain Age in the Same Way? *Frontiers in Neurology*, *12*. https://doi.org/10.3389/FNEUR.2021.645729

Resnick, S. M., Espeland, M. A., Jaramillo, S. A., Hirsch, C., Stefanick, M. L., Murray, A. M., Ockene, J., Davatzikos, M. C., & Resnick, S. M. (2009). Postmenopausal hormone therapy and regional brain volumes: the WHIMS-MRI Study. *Neurology*, *72*(2), 135–142. https://doi.org/https://doi.org/10.1212/01.wnl.0000339037.76336.cf

Rizvi, B., Narkhede, A., Last, B. S., Budge, M., Tosto, G., Manly, J. J., Schupf, N., Mayeux, R., & Brickman, A. M. (2018). The effect of white matter hyperintensities on cognition is mediated by cortical atrophy. *Neurobiology of Aging*, *64*, 25–32. https://doi.org/10.1016/j.neurobiolaging.2017.12.006

Salvadó, G., Molinuevo, J. L., Brugulat-Serrat, A., Falcon, C., Grau-Rivera, O., Suárez-Calvet, M., Pavia, J., Niñerola-Baizán, A., Perissinotti, A., Lomeña, F., Minguillon, C., Fauria, K., Zetterberg, H., Blennow, K., & Gispert, J. D. (2019). Centiloid cut-off values for optimal agreement between PET and CSF core AD biomarkers. *Alzheimer's Research and Therapy*, *11*(1), 1–12. https://doi.org/10.1186/s13195-019-0478-z

Schindler, S. E., Gray, J. D., Gordon, B. A., Xiong, C., Batrla-Utermann, R., Quan, M., Wahl, S., Benzinger, T. L. S., Holtzman, D. M., Morris, J. C., & Fagan, A. M. (2018). Cerebrospinal fluid biomarkers measured by Elecsys assays compared to amyloid imaging. *Alzheimer's and Dementia*, *14*(11), 1460–1469. https://doi.org/10.1016/j.jalz.2018.01.013

836 Schwarz, C., Fletcher, E., DeCarli, C., & Carmichael, O. (2009). Fully-Automated White Matter
837 Hyperintensity Detection with Anatomical Prior Knowledge and without FLAIR. *Lecture*
838 *Notes in Computer Science (Including Subseries Lecture Notes in Artificial Intelligence*
839 *and Lecture Notes in Bioinformatics)*, *5636 LNCS*, 239–251. https://doi.org/10.1007/978-
840 3-642-02498-6_20

841 Smith, S. M., Vidaurre, D., Alfaro-Almagro, F., Nichols, T. E., & Miller, K. L. (2019).
842 Estimation of brain age delta from brain imaging. *NeuroImage*, *200*, 528–539.
843 https://doi.org/10.1016/j.neuroimage.2019.06.017

844 Solomon, A., Kivipelto, M., Molinuevo, J. L., Tom, B., & Ritchie, C. W. (2018). European
845 Prevention of Alzheimer's Dementia Longitudinal Cohort Study (EPAD LCS): Study
846 protocol. *BMJ Open*, *8*(12), e021017. https://doi.org/10.1136/bmjopen-2017-021017

847 Suárez-Calvet, M., Karikari, T. K., Ashton, N. J., Lantero Rodríguez, J., Milà-Alomà, M.,
848 Gispert, J. D., Salvadó, G., Minguillon, C., Fauria, K., Shekari, M., Grau-Rivera, O.,
849 Arenaza-Urquijo, E. M., Sala-Vila, A., Sánchez-Benavides, G., González-de-Echávarri, J.
850 M., Kollmorgen, G., Stoops, E., Vanmechelen, E., Zetterberg, H., … Vilor-Tejedor, N.
851 (2020). Novel tau biomarkers phosphorylated at T181, T217 or T231 rise in the initial
852 stages of the preclinical Alzheimer's continuum when only subtle changes in Aβ
853 pathology are detected. *EMBO Molecular Medicine*, *12*(12), 1–19.
854 https://doi.org/10.15252/emmm.202012921

855 Subramaniapillai, S., Rajagopal, S., Snytte, J., Otto, A. R., Einstein, G., & Rajah, M. N. (2021).
856 Sex differences in brain aging among adults with family history of Alzheimer's disease
857 and APOE4 genetic risk. *NeuroImage: Clinical*, *30*, 102620.
858 https://doi.org/10.1016/J.NICL.2021.102620

859 Sudre, C. H., Cardoso, M. J., Bouvy, W. H., Biessels, G. J., Barnes, J., & Ourselin, S. (2015).
860 Bayesian Model Selection for Pathological Neuroimaging Data Applied to White Matter
861 Lesion Segmentation. *IEEE Transactions on Medical Imaging*, *34*(10), 2079–2102.
862 https://doi.org/10.1109/TMI.2015.2419072

863 Ten Kate, M., Redolfi, A., Peira, E., Bos, I., Vos, S. J., Vandenberghe, R., Gabel, S.,
864 Schaeverbeke, J., Scheltens, P., Blin, O., Richardson, J. C., Bordet, R., Wallin, A.,
865 Eckerstrom, C., Molinuevo, J. L., Engelborghs, S., Van Broeckhoven, C., Martinez-Lage,
866 P., Popp, J., … Barkhof, F. (2018). MRI predictors of amyloid pathology: Results from the
867 EMIF-AD Multimodal Biomarker Discovery study. *Alzheimer's Research and Therapy*,
868 *10*(1), 100. https://doi.org/10.1186/s13195-018-0428-1

869 Vidal-Pineiro, D., Parker, N., Shin, J., French, L., Grydeland, H., Jackowski, A. P., Mowinckel,
870 A. M., Patel, Y., Pausova, Z., Salum, G., Sørensen, Ø., Walhovd, K. B., Paus, T., & Fjell,
871 A. M. (2020). Cellular correlates of cortical thinning throughout the lifespan. *Scientific*
872 *Reports*, *10*(1). https://doi.org/10.1038/s41598-020-78471-3

873 Walsh, P., Sudre, C. H., Fiford, C. M., Ryan, N. S., Lashley, T., Frost, C., & Barnes, J. (2021).
874 The age-dependent associations of white matter hyperintensities and neurofilament light in
875 early- and late-stage Alzheimer's disease. *Neurobiology of Aging*, *97*, 10–17.
876 https://doi.org/10.1016/J.NEUROBIOLAGING.2020.09.008

877 Williams, E. J. (1959). The Comparison of Regression Variables. *Journal of the Royal*

878 *Statistical Society: Series B (Methodological)*, *21*(2), 396–399.
879 https://doi.org/10.1111/J.2517-6161.1959.TB00346.X

880 Zhavoronkov, A., Mamoshina, P., Vanhaelen, Q., Scheibye-Knudsen, M., Moskalev, A., &
881 Aliper, A. (2019). Artificial intelligence for aging and longevity research: Recent advances
882 and perspectives. *Ageing Research Reviews*, *49*, 49–66.
883 https://doi.org/10.1016/J.ARR.2018.11.003